ASTROBIOLOGY
Volume 11, Number 10, 2011

DOI: 10.1089/ast.2011.0654

A Microbial Oasis in the Hypersaline Atacama Subsurface Discovered by a Life Detector Chip: Implications for the Search for Life on Mars

Victor Parro,[1] Graciela de Diego-Castilla,[1] Mercedes Moreno-Paz,[1] Yolanda Blanco,[1] Patricia Cruz-Gil,[1] José A. Rodríguez-Manfredi,[2] David Fernández-Remolar,[3] Felipe Gómez,[3] Manuel J. Gómez,[1] Luis A. Rivas,[1] Cecilia Demergasso,[4,5] Alex Echeverría,[4] Viviana N. Urtuvia,[4] Marta Ruiz-Bermejo,[1] Miriam García-Villadangos,[1] Marina Postigo,[1] Mónica Sánchez-Román,[3] Guillermo Chong-Díaz,[5,6] and Javier Gómez-Elvira[2]

Abstract

The Atacama Desert has long been considered a good Mars analogue for testing instrumentation for planetary exploration, but very few data (if any) have been reported about the geomicrobiology of its salt-rich subsurface. We performed a Mars analogue drilling campaign next to the Salar Grande (Atacama, Chile) in July 2009, and several cores and powder samples from up to 5 m deep were analyzed *in situ* with LDChip300 (a *Life Detector Chip* containing 300 antibodies). Here, we show the discovery of a hypersaline subsurface microbial habitat associated with halite-, nitrate-, and perchlorate-containing salts at 2 m deep. LDChip300 detected bacteria, archaea, and other biological material (DNA, exopolysaccharides, some peptides) from the analysis of less than 0.5 g of ground core sample. The results were supported by oligonucleotide microarray hybridization in the field and finally confirmed by molecular phylogenetic analysis and direct visualization of microbial cells bound to halite crystals in the laboratory. Geochemical analyses revealed a habitat with abundant hygroscopic salts like halite (up to 260 g kg^{-1}) and perchlorate (41.13 $\mu g\ g^{-1}$ maximum), which allow deliquescence events at low relative humidity. Thin liquid water films would permit microbes to proliferate by using detected organic acids like acetate (19.14 $\mu g\ g^{-1}$) or formate (76.06 $\mu g\ g^{-1}$) as electron donors, and sulfate (15875 $\mu g\ g^{-1}$), nitrate (13490 $\mu g\ g^{-1}$), or perchlorate as acceptors. Our results correlate with the discovery of similar hygroscopic salts and possible deliquescence processes on Mars, and open new search strategies for subsurface martian biota. The performance demonstrated by our LDChip300 validates this technology for planetary exploration, particularly for the search for life on Mars. Key Words: Atacama Desert—Life detection—Biosensor—Biopolymers—*In situ* measurement. Astrobiology 11, 969–996.

1. Introduction

The space science community agrees on the need to explore the martian subsurface for evidence of intact organic molecules (Kminek and Bada, 2006; Shkrob *et al.,* 2010). In fact, ESA's ExoMars mission aims to search for life or its remains by analyzing samples taken from a drill hole of at least 2 m in depth (http://www.esa.int/SPECIALS/ExoMars/SEM10VLPQ5F_0.html). Dartnell *et al.* (2007) suggested, after a series of simulation experiments on the effect of solar radiation on biological material (bacteria), that a minimum depth of 7.5 m would be needed to find viable cryopreserved cells.

Different robotic missions have shown that Mars is a salty planet with a volcanic basement (Murchie *et al.,* 2009). Chlorides and bromides precipitated as cementing salts in eolian deposits (McLennan *et al.,* 2005) or likely as sedimentary deposits that infilled shallow basins (Osterloo *et al.,* 2008) due to a strong oversaturation of solutions that leached to the Mars surface under high evaporative rates. Chloride-bearing salts are excellent matrices for the preservation of biological remains (Fish *et al.,* 2002; Stan-Lotter *et al.,* 2006), and their hygroscopic properties can produce deliquescence events under low relative humidity (Davila *et al.,* 2008). In fact, the high content of perchlorate (ClO_4^-) at the Phoenix

[1–3]Departments of [1]Molecular Evolution, [2]Instrumentation, and [3]Planetology and Habitability, Centro de Astrobiología (INTA-CSIC), Madrid, Spain.
[4]Centro de Biotecnología, [5]Centro de Investigación Científica y Tecnológica para la Minería, and [6]Department of Geological Sciences, Universidad Católica del Norte, Antofagasta, Chile.

lander site on Mars (Hecht *et al.,* 2009) might promote the formation of stable liquid saline water on present-day Mars (Zorzano *et al.,* 2009).

The Atacama Desert is one of the most accurate terrestrial analogues for martian environments because it combines the formation of two key inorganic compounds: chlorides and perchlorates. Similar to events on Mars, harsh arid conditions promoted an extreme oversaturation of the ground and surface water solutions, which resulted in nearly exclusive precipitation of halite, the end member in evaporation from brines, with no other mineral phase (Chong-Díaz *et al.,* 1999). The bounding regions of the Salar Grande (Cordillera de la Costa, región de Atacama, Chile) are characterized by saline subsoils associated with nitrate deposits that contain chlorides, sulfates, chlorates, chromates, iodates, and perchlorates. These salts are older and different from those of the more central region of the Salar Grande (Chong-Díaz *et al.,* 1999).

Though the Atacama Desert has been studied for many years as a Mars analogue (Cameron, 1969; Cabrol *et al.,* 2001; Glavin *et al.,* 2004; Shafaat *et al.,* 2005; Skelley *et al.,* 2005), very few studies have focused on the microbiology or molecular biomarker content of the subsoil. Lester *et al.* (2007) described the microbiology from the surface to 15 cm deep, and Bobst *et al.* (2001) reported a 100 m drilling in the Salar de Atacama (23°S, 68°W) only for paleoclimatic studies. Gramain *et al.* (2011) described the archaeal community, identified via nested PCR and cultivation, that occupied a pure halite core up to 15 m deep from the Salar Grande. However, most of the microbiological and life-detection studies on the Atacama Desert have focused mainly on the surface or very close to it (Navarro-González *et al.,* 2003; Lester *et al.,* 2007; Weinstein *et al.,* 2008). Cabrol *et al.* (2007) used a fluorescence detection system on board a rover (Zoë) to detect fluorescent signals from biological material (*e.g.,* chlorophyll) along different transects. Piatek *et al.* (2007) used a combined orbital image analysis and a field rover with instrumentation aimed to examine the mineralogy, geomorphology, and chlorophyll potential of field sites on the surface. We did not find in the literature any systematic study that involved the search for life or traces of it or the microbiology of the Atacama subsurface below a few centimeters. Further, there have been no studies conducted in which techniques based on immunological biosensors were used.

Here, we present the results of the July 2009 astrobiological field campaign, AtacaMars2009, in which we tested a new *in situ* life-detection instrument designed for planetary exploration and study of the geomicrobiology of the Atacama subsurface at the west side of the Salar Grande. The key instrument was Signs Of LIfe Detector V3.0 (SOLID3) and its LDChip300 biosensor (a Life Detector Chip with 300 antibodies), which was designed to detect a broad range of molecular biomarkers with different specificities and sensitivities at low parts per billion levels for proteins and peptides or 10^4 to 10^5 cells per milliliter (Parro *et al.,* 2005, 2008a, 2011a; Rivas *et al.,* 2008; Parro, 2010). The LDChip300 biosensor contains antibodies against universal biomolecules like DNA, nucleotides, amino acids, and peptidoglycan, and includes antibodies that target general groups of bacteria (*e.g.,* Gram-positive cells or *Bacillus* spp. spores) and bacterial strains from different phylogenetic groups and different extreme environments (it contains a relatively high redundancy of antibodies against environmental extracts and bacterial strains from the acidic sulfur- and iron-rich environment of Río Tinto in Spain). LDChip300 also contains some antibodies that target relevant metabolic pathways.

LDChip300 detected bacteria, archaea, and molecular biomarkers, all of which were especially abundant around 2 m deep. This suggests the presence of a microbial oasis in the Atacama subsurface. The results obtained in the field were exhaustively checked and validated in the laboratory with conventional techniques, which confirmed the presence of a new subsurface hypersaline environment. The mineralogical composition together with the extremely low liquid water availability suggests important analogies with some martian environments. Our LDChip may open a new era for life-detection systems in planetary exploration.

2. Materials and Methods

2.1. Logistics, base camp, and tasks

The campaign was carried out such that it was completed by July 31, 2009, wintertime in the region. A base camp for eight researchers and two assistants was set up at about 1 km distance from the drilling site (GPS coordinates: 20°58′7.30″S, 70°2′2.95″W) (Fig. 1A). The camp included a tent that was used as a field laboratory with space for three people and some equipment (a microcentrifuge, a water bath, a scanner, a handheld sonicator, tubes, and other materials and reactants). Drilling was usually done by two people, with the assistance of two more during the more complicated operations (removing the cores, changing the corers, etc). Three people were stationed permanently in the field laboratory processing and analyzing samples, one of whom performed geophysical studies and assisted in the lab.

2.2. Drilling and sample collection

The apron at the base of a mountain of volcanic origin nearby the Salar Grande was chosen as a Mars analogue for the drilling and life-detection campaign (Fig. 1A). We measured temperature extremes of −3°C and 39°C at the drilling site during the campaign. The drilling was done with a CARDI EN 400, a 4.08–horse power gas-powered motor, and 85 mm diameter commercial off-the-shelf diamond-impregnated coring drill bits and rods. The drilling operations were difficult due to the limited power of the apparatus. To minimize cross contamination and assist drilling, compressed air was injected inside the corer to help transport chips up and out of the hole. No filtering devices were used to avoid potential contamination from the compressed air. If any contamination were to come from the compressed air, we would have detected it nearly uniformly in all core samples, which we did not. Rather, we obtained clearly differentiated patterns along the entire hole. Samples ranging from 500 g to 3 kg of this material were collected with a vacuum sampling system (a commercial aspirator with a new and sterile bag) and were labeled and stored for later analysis (Table 1). Samples were collected in plastic bags or wrapped in aluminum foil, and were then stored at room temperature (in the shade) inside closed boxes for as long as 2 h. The samples were then carried out to the field laboratory to be analyzed or further stored until transport to the laboratory in the Centro de Astrobiología, Madrid, Spain.

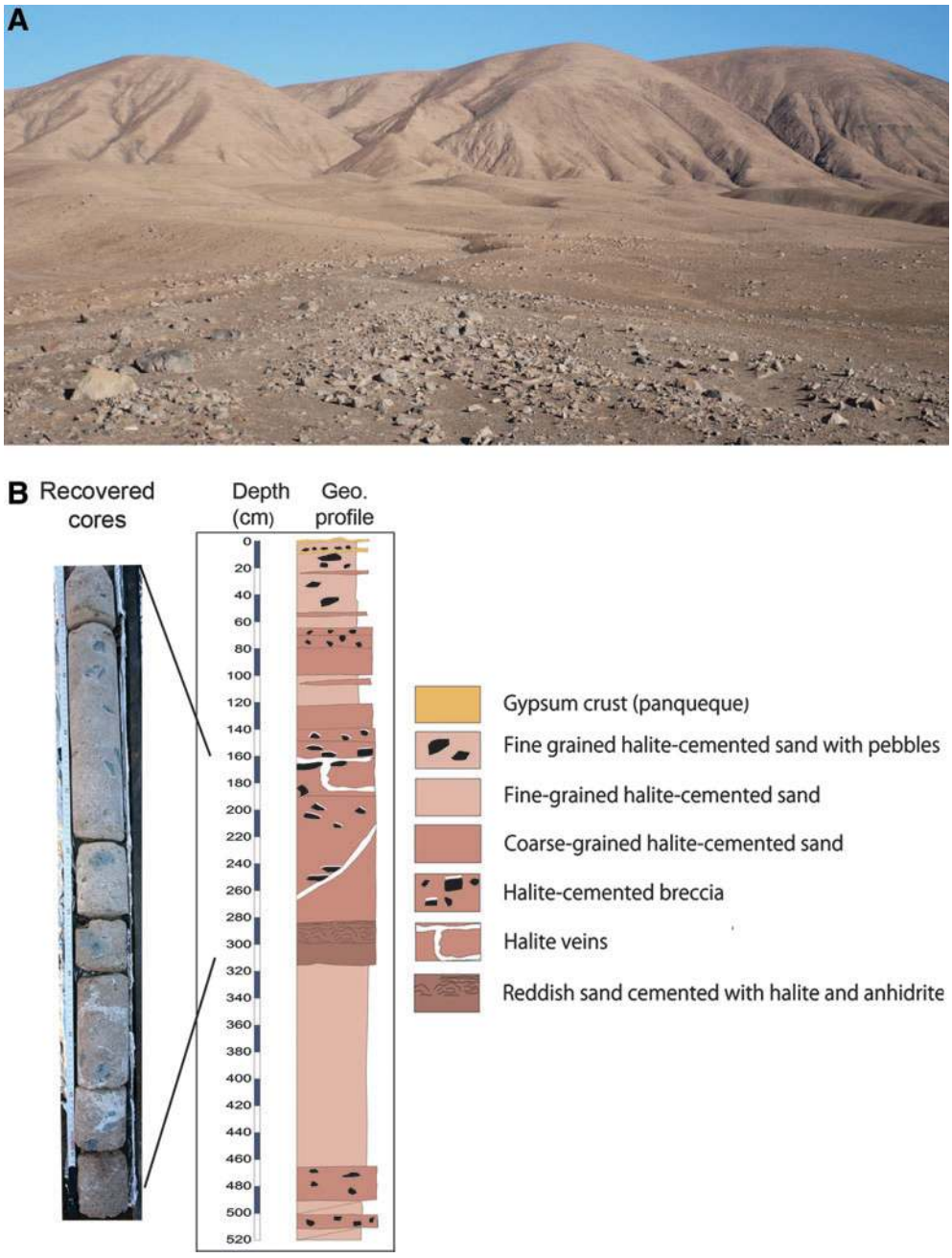

FIG. 1. AtacaMars2009 drilling campaign. (**A**) The drilling site in one apron located at the base of a mountain to the west of the Salar Grande (Atacama Desert, Chile). (**B**) Geological profile of the core with the depth scale and a photograph of the collected core pieces (left), showing the white halite veins. Color images available online at www.liebertonline.com/ast

2.3. Raman spectroscopy in the field

Intact cores were immediately photographed, analyzed with Raman spectroscopy, and then wrapped in aluminum foil to be transported to the laboratory in Spain. Raman spectra were taken in the field with a portable Avantes AvaSpec-2048TEC Raman spectrometer with $10\,cm^{-1}$ spectral resolution, a 50 mW, 532 nm diode laser, and a fiber optic probe custom-made by InPhotonics according to these parameters. The Raman excitation source, made by PD-LD, is a "Volume Bragg Grating"–stabilized module, which consists of a stabilized laser diode and the associated electronics. This module provides a high-stability output around 532 nm, with a typical spectral line width of 0.08 nm.

2.4. Antibody production, purification, and labeling

The antibodies used in this research (see Table 2 in Appendix) were the result of several years of work aimed at the detection of molecular biomarkers for planetary exploration. At the time the present study began we had a collection of 300 antibodies, which constituted the so-called immunosensor LDChip300. The criteria for antibody production and selection were explained previously by Parro *et al.*

Table 1. List of the Samples Collected during the Drilling Campaign

Sample ID	*Depth (cm)*	*Comments*
0	0–5	Chips and powder
5	5–10	Chips and powder
10	10–11	Chips and powder
20	20–25	Chips and powder
25	25–30	Chips and powder
30	30–33	Chips and powder
35	35–38	Chips and powder
40	39–40	Chips and powder
45	40–45	Chips and powder
60	60–68	Chips and powder (hard crust)
68	68–70	Stones
90	90–95	Chips and powder (hard crust)
100	100–104	Chips and powder
105	105–108	Chips and powder
110	110–112	Chips and powder
115	115–118	Chips and powder
120	120–122	Chips and powder
122	122–125	Small core
125	125–130	Small core
130	130–131	Chips and powder
131	131–134	Small core
135	135–138	Small core
140	140–142	Chips and powder
142	142–144	Stones
145	145–150	Small core
180	180–185	Chips and powder
185	185–200	Chips and powder
200	200–205	Chips and powder
216	216–220	Chips and powder
241	241–245	Chips and powder
250	250–255	Chips and powder
286	286–290	Chips and powder
296	296–305	Chips and powder
305	305–310	Chips and powder
330	330–335	Chips and powder
340	340–345	Chips and powder
350	350–355	Chips and powder
375	375–380	Chips and powder
384	384–388	Chips and powder
389	389–300	Chips and powder
391	391–395	Chips and powder
398	398–401	Powder (white)
404	404–408	Chips and powder
408	408–412	Chips and powder
431	431–433	Chips and powder (gray)
436	436–440	Chips and powder
447	447–450	Chips and powder
455	455–560	Chips and powder
460	460–465	Chips and powder (hard crust)
470	470–475	Chips and powder
489	489–499	Chips and powder (gray-brown)
507	507–508	Chips and powder (gray crust)
508	508–511	Chips and powder

(2005), Parnell *et al.* (2007), Parro *et al.* (2008a), Rivas *et al.* (2008), and Parro *et al.* (2011a). Because we are developing an instrument for use on Mars, our choice of antibodies is guided by the types of molecular biomarkers found in organisms living on Earth under similar, Mars-like conditions. Consequently, LDChip300 contains antibodies raised against whole microbial cells (archaea and bacteria), extracellular polymers, environmental extracts from terrestrial analogues for Mars or Europa, proteins and peptides from well-conserved anaerobic metabolic pathways (nitrogen fixation, sulfate reduction, nitrate reduction, etc.), exopolysaccharides (EPS), and universal molecular biomarkers like DNA, amino acids, and other biomolecules (Table 2). All the antibodies were purified by Protein A affinity purification and fluorescently labeled as reported previously by Parro *et al.* (2005) and Rivas *et al.* (2008).

2.5. Design and construction of antibody microarrays

Antibody microarrays were constructed as described by Parro *et al.* (2005) and Rivas *et al.* (2008) with some modifications, as follows: (i) we used a commercial protein printing buffer 2×(Whatman, Schleicher & Schuell, Sandford, ME, USA) and 0.02% Tween 20 as a spotting solution; (ii) printing was done in a duplicate pattern on epoxy-activated glass slides (Arrayit Corp., Sunnyvale, CA, USA) with a MicroGrid II TAS arrayer (Biorobotics, Genomic Solutions, UK). Two microarray designs were performed: one for a manual procedure for the systematic analysis of all the samples with standard microscope slides (see Section 2.6.1) and another to test the automatic procedure with the SOLID3 instrument (Section 2.6.2). For the manual procedure, up to nine identical micoarrays (9 LDChip300) containing a duplicate spot pattern for the 300 antibodies were spotted on a microscope slide so that each LDChip300 fits with one of the nine flow cells in a MultiArray Analysis Module (MAAM) device (see Section 3.1; Parro, 2010).

To test SOLID3, the microarray was also designed and constructed with a MicroGrid II TAS arrayer (BioRobotics, Digilab, Holliston, MA, USA). Five LDChip300 replicas were printed in five parallel microarrays so that they fit into the five different flow cells on the SOLID3 Sample Analysis Unit (Parro *et al.*, 2011a). Antibodies were printed at 1 mg mL^{-1} in protein printing buffer (Whatman, Schleicher & Schuell, Sandford, ME, USA) on a specially designed glass slide (dimensions $75 \times 27 \times 0.15$ mm) activated with Superepoxy chemistry (custom made by Arrayit Corporation, CA, USA).

In all cases, after printing, the antibody microarrays were kept at room temperature until used. We verified that printed antibodies were stable in printing buffer for at least one year at room temperature and could be transported to the field with no significant loss of activity (data not shown). SOLID3 was run and operated as described previously (Parro *et al.*, 2011a).

2.6. Sandwich microarray immunoassay (SMI) procedures

To analyze solid samples by SMI, the potential molecular biomarkers present in the sample have to be extracted into a liquid solution or suspension and then incubated in the presence of the capturing antibodies previously immobilized on the microarray. After a second incubation with fluorescent tracer antibodies, the positive antigen-antibody reactions are read by fluorescence emission either by CCD device or a scanner. In this campaign, we analyzed the samples by a manual procedure or automatically by using the SOLID3 instrument. Because SOLID3 is designed for single use for planetary exploration and it needs a clean room to load a new microarray chip, only five assays can be

done. Therefore, the samples were assayed by manual procedure with use of the small and portable MAAM device for nine simultaneous analyses (see Section 3.1).

2.6.1. Manual SMI using the MAAM. Immediately before use, the nine microarrays containing printed slides were treated and washed with a BSA-containing solution to block all free binding sites on the slides and to remove the excess of non-covalently-bound antibodies. For that purpose, the slides were inverted and dropped onto a 0.5 *M* Tris-HCl pH 9, 5% (w/v) bovine serum albumin (BSA) solution for 2 min and then immersed into 0.5 *M* Tris-HCl pH 8, 2% BSA solution (TBSB, Tris buffered saline–BSA), with gentle agitation for 1 h. After drying with a short centrifugation, slides were ready for immediate use to analyze samples by a sandwich immunoassay. The samples to be analyzed were processed as follows: (i) up to 0.5 g of dust or ground core samples were sonicated in 1 mL of TBSTRR buffer (0.4 *M* Tris-HCl pH 8, 0.3 *M* NaCl, 0.1% Tween 20) by using a manual sonicator for 3×1 min cycles (Dr. Hielscher 50W DRH-UP50H sonicator, Hielscher Ultrasonics, Berlin, Germany); (ii) the sonicated samples were filtered through 20-micron nylon filters to remove sand and coarse material. Then 50 μL of the filtrate was injected into one of the nine flow cells of the MAAM device to put it in contact with LDChip300, where it was left to incubate at ambient temperature (20–30°C) for 1 h with mixing by pipetting every 15 min. To attain more homogeneous conditions between different microarray incubations, we avoided extreme temperatures (−1°C to 5°C during the night or up to 35–39°C during the day) by incubating during middle morning or late afternoon, when the ambient temperature in the field laboratory was in the range of 15–30°C. Then the microarrays were washed out by passing 3–5 mL of the same buffer through the flow cells and evacuating the last volume by pipetting air. The positive antibody-antigen reactions were revealed by incubation with 50 μL of a cocktail containing 300 fluorescent antibodies at a final concentration of approximately 100 μg mL^{-1} for the whole mixture and an average around 0.4 μg mL^{-1} of each antibody. After 1 h incubation at ambient temperature, the microarrays were washed out again to remove the excess fluorescent cocktail; the slide was separated from the MAAM, rinsed by dipping into a 50 mL falcon tube filled with distilled water, and finally dried by a short centrifugation in a small and portable microcentrifuge designed for slides (Arrayit Corp.). Finally, the slides were analyzed in the field laboratory by illuminating them with 635 nm light and imaging their fluorescent emission at 650 nm with a GenePix 4100A scanner. The images were quantitatively analyzed in the field by using GenePix Pro software (Genomic Solutions) installed on a laptop computer. A blank was always run in parallel with only buffer as an "antigenic" sample and then revealed with the same fluorescent antibody or antibody cocktail as the real samples. The final fluorescence intensity (F) for each antibody spot was calculated with the equation $F=(F_{\text{sample}}-F_{\text{blank}}-3\text{Fav}_{\text{control spots}})$, where F is the fluorescent intensity at 635 nm minus the local background as quantified by the software (GenePix Pro) and where F_{sample} is the total fluorescence signal of the sample, F_{blank} the total fluorescence signal of the blank, and $\text{Fav}_{\text{control spots}}$ the average fluorescent signal of the control spots. Said control spots are located in different parts of the microarray and consist of BSA, only buffer, and others corresponding to the pre-immune antisera (more than 50). Because, theoretically, they should not exhibit any fluorescent signal, we use them as a baseline for fluorescence. We always subtract 2–3 times the $\text{Fav}_{\text{control spots}}$ as a stringency cutoff to minimize false positives. Those spots having obvious defects (missing or very tiny spots, an artifact due to a bad wash or dust in the array) or those duplicated spots whose standard deviation was 0.2 times higher than the mean were not considered for quantification.

2.6.2. Automatic SMI in SOLID3. SOLID3 is the third prototype of the SOLID (Signs Of Life Detector) instrument concept devoted to the detection of molecular biomarkers in planetary exploration (see Section 3.1). It is an analytical instrument, based on antibody microarray technology, that can detect a broad range of molecular-sized compounds, from the amino acid size level to whole cells, with sensitivities at 1–2 ppb (ng mL^{-1}) for biomolecules and 10^4 to 10^5 cells mL^{-1} (Fernández-Calvo *et al.*, 2006; Rivas *et al.*, 2008; Parro *et al.*, 2011a). SOLID3 is currently in Technology Readiness Level (TRL) 5–6, although some of the internal elements are in the TRL 9 stage (Parro *et al.*, 2011a). The instrument accepts both solid (dust or ground rock or ice) and liquid samples. The limit of sample volume ranges from 0.5–1 cm^3 to 2.5 cm^3 (mL) at final processing volume (including the extraction buffer supplied by the instrument). SOLID3 is able to perform both sandwich and competitive immunoassays and consists of two separate functional units: a Sample Preparation Unit (SPU) for 10 different extractions by ultrasonication, and a Sample Analysis Unit (SAU) for fluorescent immunoassays. The SAU consists of five different flow cells, with an antibody microarray LDChip300 in each one. It is also equipped with an exclusive optical package and a CCD device for fluorescence detection.

After loading up to 0.5 g of dust or ground core sample into one of the homogenizing chambers of SOLID3's SPU, the instrument was set to run autonomously as described in Parro *et al.* (2011a). After being started, SOLID3 adds 2 mL of extraction-incubation buffer, TBSTRR, to the homogenizing chamber. A sonicator horn pushes a ring membrane forward, hermetically closing the chamber, and advances to the sonication position. After four cycles of sonication, the linear actuator pushes the sample forward through a filtering system (15 μm pore size). The filtrate is injected into the SAU, floods one of the flow cells, and contacts one of the LDChip300 antibody microarrays. An internal recirculation circuit allows the sample to be re-circulated for up to 1 h in order to enhance the reaction kinetics between antigens and spotted antibodies. After the incubation time, the remaining sample is discarded into the waste deposit, and the microarray cell is washed out with the incubation buffer to remove the nonbound sample. Then the buffer is injected into the auxiliary chambers that are pre-loaded with a cocktail of 300 lyophilized fluorescent antibodies. The buffer dissolves the antibodies and floods the microarray chamber, where it is recirculated for up to 1 h. An additional wash removes the excess of fluorescent antibodies and leaves the microarray ready for fluorescent detection by excitation with a laser beam via total internal reflection through the glass support, which acts as a waveguide. The fluorescent signal is captured by a highly sensitive CCD detector and stored as a Flexible Image Transport System (*i.e.*,*.fits) image file that can be

processed and analyzed by conventional microarray software as described in Section 2.6.1. One of the microarrays is incubated with only the buffer (blank) and revealed with fluorescent antibodies. The blank image is used as a baseline to calculate spot intensities in the tested sample, as described in Section 2.6.1.

2.7. Environmental DNA extraction and PCR amplification

Total DNA was extracted from 2 g of sample (powder or ground cores) by using the commercial DNA EZNA soil DNA kit (Omega Bio-Tek, Inc., Norcross, GA, USA) with some modification: after cell lysis, the extract was partially desalinated by using Amicon 30 filters (Millipore) following the manufacturer's protocol. We used the obtained DNA for simultaneous fluorescent labeling and PCR amplification by using the bacterial universal primers for 16S rRNA gene 16SF as forward (positions 8–27 of *Escherichia coli* 16S rRNA, 5′-AGAGTTTAGTCATGGCTCA) and 16SR as reverse (positions 1057–1074, 5′-CACGAGCTGACGACAGCCG). The reactants were previously set up in a gelified mixture (Biotools S.A, Madrid, Spain) containing the buffer, the nucleotide precursors, the fluorescent nucleotide Cy3-dUTP, the primers, and the enzyme as follows: 10×buffer (5.0 μL), 50 m*M* $MgCl_2$ (3.0 μL), 10 m*M* dACTPs (0.5 μL), 1 m*M* dTTP (6.25 μL), 2 nm/μL Cy3-dUTP (5.0 μL), forward primer 10 m*M* 16SF (1.0 μL), reverse primer 10 m*M* 16SR (1.0 μL), Taq-platinum 5U/μL (Invitrogen) (1.0 μL), and distilled H_20 (27 μL). The gelification process was carried out by Biotools S.A. (Madrid, Spain). The samples prepared in this way can be stored for long periods at ambient temperature. Additionally, we prepared PCR mixtures without fluorescent nucleotides: 10×Buffer (5.0 μL), $MgCl_2$ 50 m*M* (1.5 μL), dNTPs 10 m*M* (1.0 μL), primer 16SF 10 m*M* (1.0 μL), primer 16SR 10 m*M* (1.0 μL), Taq-platinum 5U/ul (1.0 μL), and dH_20 (40 μL). Gelified samples were reconstituted by adding distilled nuclease-free water and the template DNA. For simultaneous labeling and PCR amplification, the field thermocycler was programmed as follows: 95°C, 5 min; 10×(95°C 20 s, 50°C 30 s, 68°C 60 s); 25×(95°C 20 s, 48°C 30 s, 68°C 60 s+5 s per cycle); 68°C 10 min; 4°C.

2.8. Oligonucleotide microarray hybridization in the field laboratory

Oligonucleotide microarrays containing specific probes for prokaryotic microorganisms, like our previously reported prokaryotic acidophile microarray (PAM), were printed and treated as described by Garrido *et al.* (2008). This microarray was specially developed for the detection of prokaryotic acidophiles in several field campaigns to the extremely acidic environment of Río Tinto (Huelva, Spain), but it also contains specific oligonucleotide probes for the 16S and 23S rRNA genes from other universal groups: Alpha-, Beta-, Gamma-, and Deltaproteobacteria, as well as Firmicutes (low GC content), high-GC-content Gram-positive bacteria, Archaea, and so on. Fluorescently labeled 16S rRNA gene amplicons were checked by agarose gel electrophoresis then purified with Qiagen PCR purification kit columns (Qiagen, CA, USA) and set to hybridize in HibIt hybridization buffer (Arrayit Corp.) at 50°C for 12 h in a water bath. They were then washed and scanned for fluorescence as previously described (Garrido *et al.*, 2008). Because the probes for Beta- and Gammaproteobacteria correspond to sequences from the 23S rRNA gene and we used only the amplicon from 16S rRNA gene for fluorescent labeling, we could not detect these types of bacteria in hybridization with the oligonucleotide microarray.

2.9. Determination of total protein and sugar content in the field laboratory

Total protein and sugar content in the samples was determined in the field laboratory as follows: 1 g of sample (powder) was subjected to 3×1 min ultrasonication cycles in 2 mL of distilled water with 1–2 min stops by using a handheld sonicator (Dr. Hielscher 50W DRH-UP50H sonicator, Hielscher Ultrasonics, Berlin, Germany). Samples were centrifuged at 2000*g* to sediment the mineral particles, and the supernatants were directly assayed for protein concentration by using the bicinchoninic acid protein assay reagent (Pierce, Rockford, IL, USA) (Smith *et al.*, 1985) and sugar content as described by Dubois *et al.* (1956), respectively. A NanoDrop (NanoDrop Int.) instrument was used for spectrophotometric measurements.

2.10. Agarose gel electrophoresis

For DNA fractionation and visualization a pre-stained agarose gel and a portable FlashGel System (Cambrex, East Rutherford, NJ, USA) were used and run following the manufacturer's recommendations. A personal digital camera (Panasonic) was used to take pictures of the gel.

2.11. Phylogenetic analysis by cloning and sequencing of the bacterial 16S rRNA gene

The extracted environmental DNA was used as template for PCR amplification of the bacterial 16S rRNA gene with the primer pair 16SF-16SR. The product from this reaction was used as template for a second PCR amplification with primers 63F (positions 43–63, 5′CAGGCCTAACACATGCA AGTC) and 907R (positions 906–926, 5′-CCGTCAATTCM TTTGAGTTT). The amplicon was cloned into vector pTOPO-TA (Invitrogen) and sequenced from both ends in an ABI 3710 automatic sequencer (PE Biosystems, General Electrics). Sequences were assembled with the package Phred-Phrap-Consed, with use of a Perl wrapper that automatically clustered and processed the chromatograms corresponding to individual clones (Ewing *et al.*, 1998; Gordon, 2004). Putative chimeras were discarded after screening the assembled clone sequences with Bellerophon (Huber *et al.*, 2004). The remaining clone sequences were assigned to taxonomical categories with use of the Ribosomal Database Project (RDP) web server (Cole *et al.*, 2009). Complementary taxonomical information was obtained by comparing the clone sequences against the NCBI NR database with BLAST (Altschul *et al.*, 1997). The alignments generated by RDP were used as input for Mothur application (Schloss *et al.*, 2009) to calculate distance matrices ignoring terminal gaps, cluster clone sequences into operative taxonomical units (OTUs), generate rarefaction curves, identify OTUs shared across samples, and calculate the Ace and Chao1 estimators for species richness and the Simpson Index (D) for community diversity.

2.12. Phylogenetic analysis by cloning and sequencing of the archaeal 16S rRNA gene

For archaeal 16S rRNA gene amplification, two rounds of PCR amplification were performed with the universal archaeal primer pair 21F-958R (Delong, 1992) for the first round and the specific pair for the domain Archaea ARC344F-ARC915R (Stahl and Amann, 1991) for the second round. The thermocycler was programmed as follows: 94°C, 7 min; 30×(94°C, 1 min; 56°C, 1 min); 72°C, 7 min; 4°C for the first round, and 94°C, 4 min; 10×(94°C, 1 min; 68°C – 1°C per cycle, 1 min; 72°C, 1.5 min); 20×(94°C, 1 min; 60°C, 1 min; 72°C , 1.5 min); 72°C, 30 min; 4°C, for the second round. We used the Go-Taq Green master mix and the GoTaq polymerase (Promega Corp., WI, USA) in a 50 μL final reaction volume.

2.13. DAPI staining

To visualize cells with optical microscopy, the microorganisms from the ground samples were separated from the inorganic and humic fractions with physical dispersion techniques, such as low- and high-speed centrifugation. Two 5 g aliquots of the samples analyzed by DAPI were resuspended in 50 mL of extraction buffer (1.5 *M* NaCl, 0.15% Tween 20, 10 m*M* Tris pH8, and 100 m*M* EDTA), then incubated for 2 h at room temperature in a roller and subsequently centrifuged at 2000*g* for 2 min. The pellet, which consisted mainly of minerals and coarse material, was discarded, and the supernatant was centrifuged at 10,000*g* for 10 min. The resulting new pellet was washed in 300 μL of the extraction buffer and centrifuged at 15000*g* for 5 min. The supernatant was discarded, and a few cells were collected with a sterile loop-spreader from the upper section of the wet pellet, spread on a microscope slide, left to dry, and incubated with 5 μL of 1 μg mL^{-1} DAPI-blue stain solution for 1 min. The slide was rinsed with water and then with 80% ethanol to remove the non-specific-bound DAPI stains. Cells were visualized in an Olympus Bx40 microscope at ×100 augmentations. Images were captured with an Olympus DP70 camera. Additionally, small pieces of core samples were subjected to a quick stain with DAPI in an Eppendorf tube, washed with buffer, and observed directly under the microscope. Under these conditions, we visualized cells with flagellar movement.

2.14. Biochemical extractions

Extracts were prepared from 20 to 40 g of different samples with GuHCl buffer (4 *M* guanidine-hydrochloride, 0.5 *M* EDTA, 0.5 *M* Tris pH 7.4) following the procedure described by Tuross and Stathoplos (1993). The final extracts were resuspended in sterile distilled water, dialyzed (>1200 Da cutoff) against water, and finally lyophilized. These extracts were used for the identification of amino acids by gas chromatography–mass spectrometry (see Section 2.15).

2.15. Determination of amino acids

For the identification of amino acids, the samples were first hydrolyzed with 6 *M* HCl at 110°C for 24 h and then freeze-dried to remove water, HCl, and any volatile organics. The hydrolyzed samples were analyzed, in a way similar to that described by Ruiz-Bermejo *et al.* (2007), by high-pressure liquid chromatography after derivatization with phenylisothiocyanate (Thermo-Fischer) with use of the following conditions: Solvent A: 50 m*M* NH_4OAc buffer, pH 6.5; Solvent B: 100 m*M* NH_4OAc-CH_3CN (50:50), pH 6.5; 0 min 0% B (100% A), 45 min 70% B (30% A), 46 min 70% B (30% A), 48 min 100% B (0% A). The flow was 2 mL min^{-1}, the column was thermostated at 52°C, and the chromatogram registered at 254 nm. High-pressure liquid chromatography analyses were carried out on a Surveyor (ThermoFinnigan, Scientific Instruments Services, Ringoes, NJ, USA) with a photodiode array detector with a Kromasil 100 C_{18} 5 μm 25×0.46 column. The identifications of the amino acids were verified by comparing the retention times and UV absorbance spectra with external standards, purchased from Sigma-Aldrich and Fluka (Sigma-Aldrich, St. Louis, MO, USA).

2.16. Determination of total organic carbon

Up to 2 g of sample were dried by incubating at 110°C for 24 h. Total organic carbon was estimated by the weight of sample lost after a second incubation at 550°C for 3 h.

2.17. Testing the deliquescence properties of the drilled samples

To test the capacity of the collected samples to absorb and deliquesce atmospheric water vapor, we proceeded as follows: 2 g of samples was exhaustively dried at 110°C for 24 h (until no further weight loss was measurable); then they were stored in identical 100 mL glass beakers covered by aluminum foil (ajar) in a cold room at 4°C and below 75% relative humidity. Over the next 20 days, the samples were weighted daily. The water-weight gain was plotted as the percentage of the initial dried weight. Deliquescence, defined as the process by which a substance absorbs moisture from the atmosphere until it dissolves in the absorbed water and forms a solution, was clearly visible to the naked eye. Some of the samples even showed liquid water accumulating at the bottom of the beaker after only 5 days.

2.18. Ion chromatography analysis

Samples (10 g) were sonicated (3×1 min cycles) in 20 mL of water, and the mineral particles were removed by centrifugation. The supernatants were collected and loaded into a Metrohm 861 Advanced compact ion chromatographer IC (Metrohm AG, Herisau, Switzerland) undiluted or at dilution values of either 50% or 20%. For all the anions, except perchlorate, the column *Metrosep A supp 7-250* was used with 3.6 m*M* sodium carbonate ($NaCO_3$) as eluent. For perchlorate measurements, we used a *Metrosep A supp 4-250* column with 1.9 m*M* Na_2CO_3, 1.9 m*M* $NaHCO_3$, 25% (w/v) acetonitrile as eluent. The pH of the water solutions was measured with an inoLab pH meter (WTW, GmbH & Co. KG, Weilheim, Germany) after 24 h of solution stabilization.

2.19. Scanning electron microscopy (SEM)

Scanning electron micrographs were made with gold-coated pieces of core samples by using a JEOL JSM-5600 LV instrument (JEOL, Tokyo, Japan). To examine the micromorphology and mineralogy, it was operated at acceleration voltages of 10–20 kV and 2–3 kV. The phase compositions were measured by using energy-dispersive X-ray (INCA

X-Sight, Oxford), with acceleration voltages of 10 kV for minerals and 2 kV for microorganisms.

3. Results

3.1. *LDChip300 detected* in situ *microbial biomarkers in the Atacama subsurface*

A 1-week duration drilling campaign was carried out in the apron at the base of a mountain to the west of Salar Grande (Materials and Methods; Fig. 1). We drilled a 5.2 m deep hole (reported here) and another one of 75 cm to the east of Salar Grande (not shown). More than 40 samples that contained the chips and came up and out of the hole were collected. Additionally, several intact core pieces from 160 to 310 cm deep were also recovered (Fig. 1B). This 1.5 m of solid core corresponded to several hard layers of solid material. The rest of the core mostly corresponded to soft or weakly cemented material, except approximately 1 m that we lost at the bottom of the hole (from approx. 4 to 5.20 m) when we finished the drilling operations. The loss of this core was due to a failure in the clamping system in the corer tip. The geological profile of the whole core showed thin gypsum crusts at the upper parts followed by fine-grained halite-cemented sand layers with and without pebbles (Fig. 1B). The recovered strongly compacted cores contained halite-cemented breccia and halite veins. These samples were analyzed with a field-portable Raman spectrometer rendering spectra with peaks identified as halite and anhydrite ($CaSO_4$) crystals (Fig. 2).

Forty powder- and chip-containing samples recovered from the core (from 0 to −5 m) were analyzed in the field by fluorescent sandwich antibody microarray immunoassay with LDChip300 (Figs. 3 and 4; see Materials and Methods). The fluorescent signal of each of the 300 antibodies (Fig. 3) was quantified and plotted, which generated an immunogram from each sample (Fig. 4). Positive reactions were identified with several antibodies in several samples. Especially significant were those taken at depths around 2 m (samples **185**, **200,** and **216**), where positive reactions corresponded to antibodies raised against environmental biochemical extracts, microbial extracts, and biological compounds like DNA, EPS, or lipoteichoic acid polymers from Gram-positive bacteria, and others (Fig. 3 and Table 3). Among the microorganisms, we detected Gram-negative Alphaproteobacteria (weak signal from an Acetobacteraceae) and Gammaproteobacteria (*Acidithiobacillus, Halothiobacillus*, and Pseudomonadaceae), Gram-positive Actinobacteria and Firmicutes (Bacillales), Bacteroidetes, and the archaeon *Halorubrum* spp. The LDChip results confirm that complex polymers (EPS and lipoteichoic acids) were present in the analyzed samples, which, in turn, constitutes direct evidence of viable life or the remains of recently viable life with abundances especially high at ∼2 m. A strong fluorescent signal was obtained with an anti-steroid antibody in most of the samples below 2 m. We hypothesize that organomineral complexes bearing structurally similar compounds produced either by bacteria or fungi may have been responsible for such a high signal. A likely candidate was ergosterol, a triterpene lipid that forms part of the fungal cell membranes and functions like cholesterol in animal cells (Weete *et al.*, 2010). To verify the authenticity of the antigen-antibody reactions, some samples were heated over a flame in sterile aluminum foil for 10 min in the field laboratory and then analyzed with LDChip300. Most (at least 90%) of the fluorescent signals disappeared from the immunograms, which indicates that the signals detected in the biochip were indeed a consequence of a sandwich immunoassay against organic (most probably biological) complex polymers.

3.2. *Biochemical and molecular analyses in the field supported the LDChip300 results*

We successfully extracted DNA from two out of eight samples assayed in the field: one from the surface (sample **0**) and the other from a depth of 2 m (sample **200**). The last one also had the strongest molecular biomarker signals obtained with LDChip300 (Figs. 3 and 4). The failure in obtaining DNA from the other samples may have been due to a lower number of cells. The obtained DNA was checked

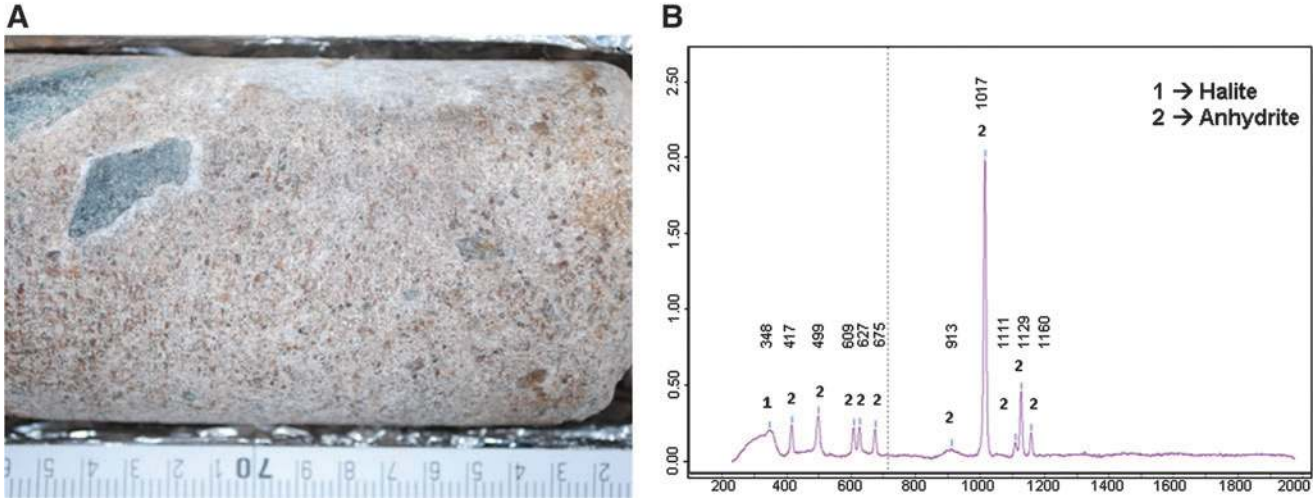

FIG. 2. Raman spectroscopy identified anhydrite and halite in the field. (**A**) Detailed image of one of the cores used for Raman analysis. (**B**) A characteristic Raman spectrum showing halite (NaCl) and the other abundant mineral, anhydrite ($CaSO_4$). Color images available online at www.liebertonline.com/ast

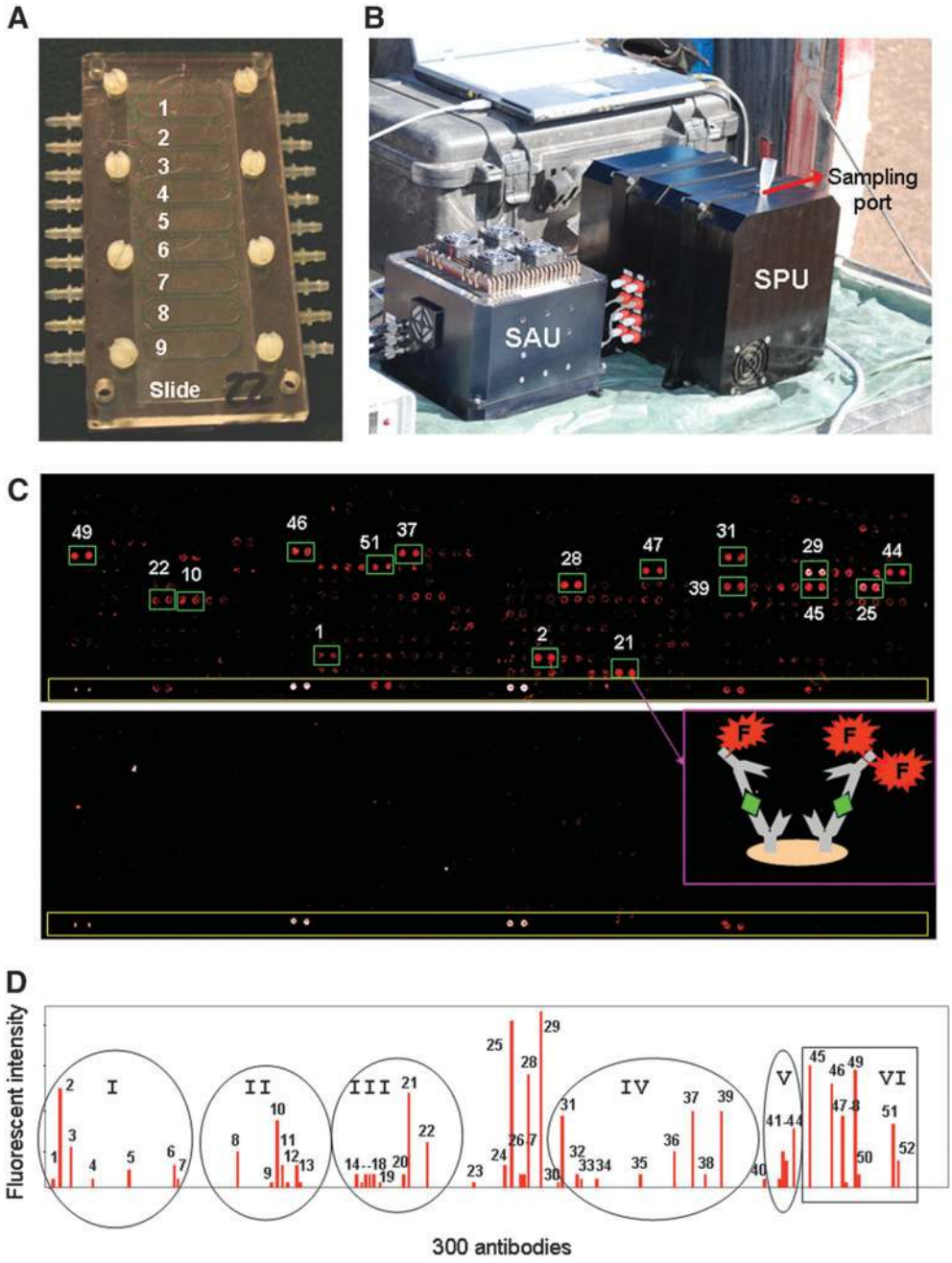

FIG. 3. LDChip300 detected microbes and polymeric biological remains at 2 m deep under the Atacama surface. (**A**) A picture showing the nine flow cells for nine simultaneous LDChip300 assays in the MAAM device (see Section 2.6.1). (**B**) A picture of the SOLID3 instrument in the field, showing its two functional units: the Sample Preparation Unit (SPU) and the Sample Analysis Unit (SAU) (See Section 2.6.2). (**C**) LDChip300 image obtained with sample **200** (*top*) indicating some of the spots with the highest fluorescent signals. The cartoon shows how capturing antibodies (Y forms) bind biological polymers (rhombi) and how they are sandwiched by fluorescent (F) tracer antibodies. The image obtained with the negative control (*bottom*) was used as a baseline (blank) to calculate spot intensities in the test samples. Long yellow rectangles encompass a fluorescent spot gradient. (**D**) Immunogram showing the fluorescence intensity of the positive spots. The peak numbers, antibody name, and immunogen can be seen in Table 3 (see also Table 2). Circles and squares indicate the main antibody clusters: (I) antibodies against whole extracts from sediments, biofilms, and water from Río Tinto rich in Gammaproteobacteria; (II) Gammaproteobacteria (*Halothiobacillus* spp., *Acidithiobacillus* spp.); (III) *Desulfosporosinus, Pseudomonas, Salinibacter;* (IV) different peptides and proteins; (V) cell wall polymeric components like lipoteichoic acids, lipidA, or peptidoglycan; (VI) nitroaromatic compounds and nucleotide derivatives. Color images available online at www.liebertonline.com/ast

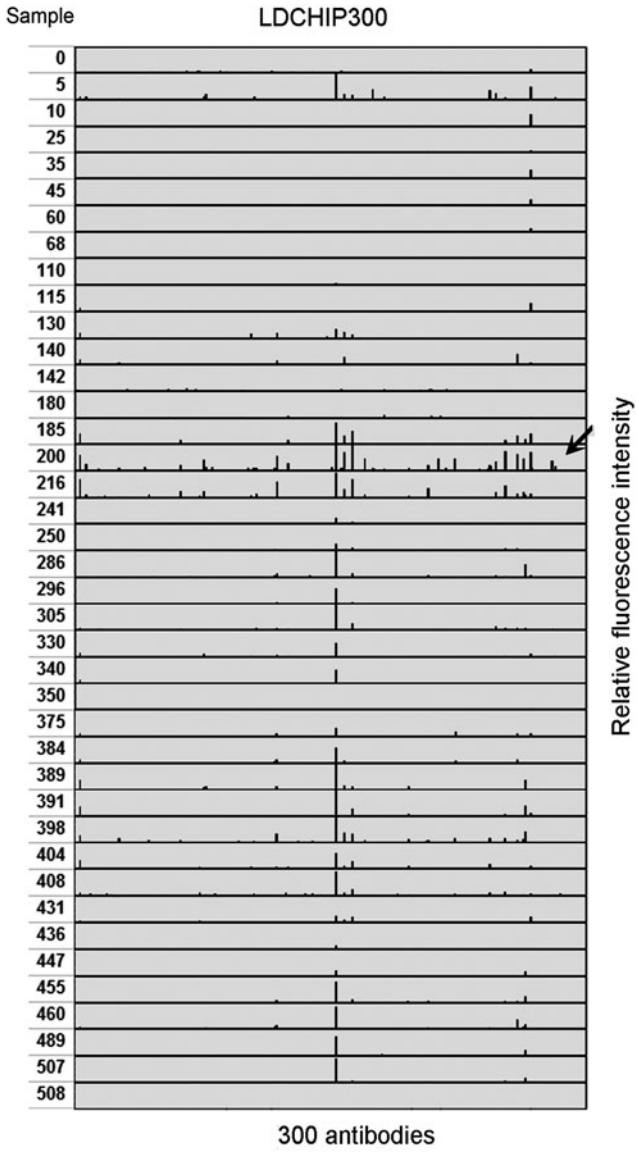

FIG. 4. LDChip300 immunoprofiling identified a new habitat in the Atacama subsurface. Ordered immunograms obtained after analyzing samples from different depths with LDChip300. The arrow indicates sample **200**, collected at 2 m deep. Note that the most abundant and intense fluorescent signals are in and around this sample (see Fig. 3 and Table 3 for details). See also text for explanation.

spectrophotometrically and by using PCR amplification of the 16S rRNA gene with bacterial and archaeal universal primers (See Sections 2.11 and 2.12, Materials and Methods). Additionally, the PCR amplicon from sample **200** was fluorescently labeled and used to hybridize to an oligonucleotide microarray designed for the analysis of prokaryotic diversity (Garrido *et al.,* 2008). The results further confirm the presence of bacteria, mainly from the Gram-positive low-GC-content Firmicutes group, as well as from the high-GC-content Gram-positive bacteria (Fig. 5 and Table 3). Total protein and sugar contents were also determined in the field laboratory, showing a peak in the samples around 2 m deep (Fig. 6), which is in agreement with LDChip300 and DNA microarray analyses, although sugars still remain high to the bottom of the hole. All these data support and validate the *in situ* LDChip300 results and are consistent with the presence of a subsurface microbial habitat.

3.3. Geochemical analyses revealed a hypersaline habitat in the Atacama subsurface

The analysis of all powder- and chip-containing samples collected during drilling by ion chromatography showed a specific geochemical pattern at around 2 m deep (Fig. 6), which is in agreement with the results obtained in the field. A slight decrease in the pH of water solutions is coincident with a high increase of salt content (NaCl) and conductivity, both decreasing just when nitrates, perchlorates, and formate contents increase and remain steady down to the bottom of the borehole (5.2 m). In contrast, sulfate content is slightly higher in the first 2–3 m. A peak of total protein and sugar profiles is consistent with the salinity (halite), conductivity, the maximal deliquescence capacity, and LDChip300 results, while the pH of the water solution used for ion chromatography analysis (Section 2.18) showed a small acidification. This subsurface habitat is characterized by the presence of high amounts of nitrates, sulfates, and perchlorates, all of which are capable of working as electron acceptors for bacterial respiration. The presence of small organic acids is also highly remarkable, with propionate and acetate dominating in the upper part, while formate increases from 2 m deep (Fig. 6). All of them can be used as electron donors to support bacterial nitrate, sulfate, and perchlorate reduction. Additionally, amino acids were also detected by gas chromatography–mass spectrometry in polymeric material extracted with guanidine-hydrochloride buffer (see Section 2.14, Materials and Methods) from different depths (Table 4). These amino acids may come either from extracellular or intracellular fractions because we cannot rule out the cell lysis with the extraction method used.

3.4. Microscopy and molecular phylogeny confirmed the presence of bacteria and archaea in the Atacama subsurface

Further analyses in the laboratory were performed to obtain new information and to validate the results obtained in the field. Core samples were assayed for microscopic evidence of cells either by SEM or optical microscopy. The scanning electron microscope images (Fig. 7) show the presence of cellular and biofilm morphologies together with mineralized cellular moulds excavated in the halite, which has a high signal for organic carbon. Fluorescent DNA-specific staining (DAPI) and microscopy analysis revealed the presence of cells with different morphologies: coccoid-, rod-, and comma-shaped, and vibrioid (Fig. 8A). After addition of water to the sample, some of these cells showed flagellar movement under the microscope, with and without a quick DAPI staining (see Section 2.13). These cells were metabolically active probably due to the water captured by the core during transport and storage in a cold room.

Phylogenetic analyses of the bacterial 16S rRNA gene (Fig. 8B) indicated that the most abundant clones found at 2 m deep were closely related to the Gammaproteobacteria class (most of them *Vibrio* spp. and some *Pseudomonas* spp.). Additionally, many clones corresponded to the phylum

Table 3. LDChip300-Detected Microbial Compounds at 2 m Deep

	LDChip300			
Phylum/group	*No. Antibody*	*Immunogen (See also Table 2)*	*PAM (16 S)*	*16S rRNA seq.*
Gamma-proteobacteria	1 IA1C1	3.2 damp water cellular fraction (Gamma, Nitrospira)		Gammaproteobacteria
	2 IA1S1	3.2 damp water supernatant		Vibrionaceae
	3 IA2S1	Green filaments EPS (Eukaryotes, Gamma …)		Xanthomonadaceae
	4 IC1C1	3.2 beach cells (Nitrospira, Gamma)		
	5 IC6C1	3.1 beach under-crusts cells		
	6 ID1C1	Jarosite Nac. Cells (Gamma, Nitrospira, others)		
	7 ID1C3	Jarosite Nac. Sonicated Cells after EDTA		
	8 IVE3C1	*Acidithiobacillus ferrooxidans* intact cells		
	9 IVE6C1	*A. caldus*		
	10 IVE7C1	*Halothiobacillus neapolitanus*		
	12 IVF2C1	*Shewanella gelidimarina* (marine broth 15°C)		
	13 IVF2S2	*S. gelidimarina* (Alteromonadaceae)		
	21 IVI1C1	*Pseudomonas putida* (Pseudomonadaceae)		Pseudomonadaceae
	23 IVI6C3	*Azotobacter vinelandii* (Pseudomonadaceae)		
Alphaproteobacteria	14 IVG1C1	*Acidocella aminolytica* (Acetobacteraceae)		
	15 IVG2C1	*Acidiphilium* spp.		
Actinobacteria	11 IVE8C1	*Acidimicrobium ferrooxidans*	HGC_G+	Actinobacteria
Firmicutes	20 IVI19C1	*Desulfosporosinus meridiei* (Clostridiales. G+SRB)	LGCa_G+	Firmicutes
	28 Lmo	*Listeria monocitogenes* (Bacillales, Listeriaceae)	LGCb_G+	Bacillaceae
	26 G+Bact	Gram+ LTA (crossreacts Bacillales)	LGCc_G+	Paenibacillaceae
	19 IVH1C1	*Bacillus subtilis* spores (Bacillaceae)		Lactobacillaceae
	43 LTA	LTA, *L. monocitogenes* (Bacillales, Listeriaceae)		Leuconostaceae
Acidobacteria	16 IVG3C1	*Acidobacterium capsulatum* (Acidobacteria)		
Deinococcus	17 IVG4C1	*Thermus scotoductus* (Deinococci-Thermales)		
	18 IVG4C2	*T. scotoductus*		
Bacteroidetes	22 IVI21S1	*Salinibacter ruber* PR1 (Bacteroidetes)		
Euryarchaeota	24 IVJ8C1	*Halorubrum* spp. (Halobacteriaceae)		*Halorubrum* spp.
Epsilonproteobac.	27 Hpyl	*Helicobacter pylori* (Gram-negative epsilon div.)		
Nucleic acids and derivatives	29 dsDNA(hu)	dsDNA (Human plasma)		
	46 cGMP(bio)	cGMP-2′-succi-BSA		
	49 cGMP(ups)	cGMP-BSA		
	50 GMP_N	GMP-BSA		
	51 cAMP_sh	cAMP-BSA		
	52 Thiamine	Thiamine-BSA		
Cell wall	41 EPS_SP	EPS Santa Pola (Alicante, Spain)		
	42 Lectin	Lectin potato specific for NAG-NAM oligomers		
	44 LipidA	LipidA (monoclonal Ab, clon 43)		
	25 Cortisol	Cortisol-17-BSA		
	47 Digoxin	Digoxin (monoclonal Ab, mouse)		
Xenobiotics	45 Atrazine	Atrazine-BSA		
	48 DNP	Dinitrophenol-BSA		

(*continued*)

Table 3. (Continued)

	LDChip300			
Phylum/group	*No. Antibody*	*Immunogen (See also Table 2)*	*PAM (16 S)*	*16S rRNA seq.*
Peptides	30 ApsA	Adenylylsulfate reductase peptide (*Desulfovibrio desulfuricans*)		
	31 ASB_prot	Bacterial ATPsynthase F1 subunit Alpha (prot)		
	32 Beta-Glu	Beta-glucanase (*E. coli*)		
	33 CcdA	CcdA peptide (Cytochrome biogenesys. *Geobacter)*		
	34 DhnA	DhnA (Dehydrin) peptide (*Nostoc*)		
	35 Hsp70	Chaperon Hsp70 (*M. tuberculosis*)		
	36 ModA	Molibdate transport peptide (*Leptospirillum ferrooxidans*)		
	37 NifH2	NifH nitrogenase peptide (*L. ferrooxidans*)		
	38 NorB	NorB protein (*Nitrobacter hamburgensis*)		
	39 Pfu_fer	Ferritin (*Pyrococcus furiosus*) protein		
	40 Stv	Streptavidin		

List of the antibodies showing positive reaction in LDChip300 with sample **200** and comparison to the results obtained with oligonucleotide microarray (PAM) in the field, and by cloning and sequencing of the 16S rRNA gene in the laboratory.

Column **No**. indicates the number of each of the peaks of the immunogram in Fig. 3. The column **PAM (16S)** indicates the group of bacteria detected after fluorescent hybridization of bacterial 16S rRNA gene in the field: HGC_G+, high-GC-content Gram-positive bacteria; LGCa,b,c_G+, low-GC-content groups a, b, and c of Gram-positive Firmicutes (see Fig. 5). Alpha, Beta, Gamma: division of proteobacteria. LTA, lipoteichoic acids. EPS, Exopolysaccharides. dsDNA, double-stranded DNA. cGMP and cAMP, cyclic guanine and adenine monophosphate nucleotides, respectively.

Firmicutes (most of them *Bacillus* spp.), and others from the phylum Actinobacteria (*Microbacterium* spp.). These results are again consistent with those obtained with LDChip300 (Table 3), where the antibodies show positive reactions that can be grouped into Gammaproteobacteria (*Shewanella, Pseudomonas,* strains or natural extracts enriched in these types of microorganisms like *Acidithiobacillus, Halothiobacillus,* and environmental extracts from Río Tinto), the Gram-positive Firmicutes, and Actinobacteria. Additionally, we obtained several sequences closely related to the archaeal genus *Halorubrum*. Again, this result is in agreement with LDChip and corroborated the first report about archaea in the Atacama subsoil.

4. Discussion

4.1. LDChip300 detected microbes and molecular biomarkers in the Atacama subsurface

We previously described the performance of former versions of LDChip (Parro *et al.,* 2008b; 2011a, 2011b; Rivas *et al.,* 2008). Herein, we demonstrate the unprecedented capacity of an immunosensor chip for the detection of microbes and molecular biomarkers in the subsurface of one of the best Mars analogues on Earth: the Atacama Desert (Fig. 3). Samples were immediately analyzed in the field after their collection from the core. Thirty samples can be assayed simultaneously with LDChip300 and the results obtained after 3 h, which allowed us to perform nearly real-time monitoring. It was highly relevant that several positive reactions obtained around 2 m deep corresponded to antibodies against Gram-positive bacterial antigens from the group Firmicutes (Table 3). This is the case for IVI19C1, raised against *Desulfosporosinus meridiei* (Clostridiales, Gram-positive sulfur-reducing bacteria); Lmo, for *Listeria monocitogenes* (Bacillales, Listeriaceae); G+Bact, Gram-positive lipoteichoic acids (cross reacts with Bacillales); IVH1C1, for *Bacillus subtilis* spores (Bacillaceae); or LTA, for LTA from the Gram-positive bacterium *Listeria monocitogenes* (Bacillales, Listeriaceae). The presence of bacteria from the Firmicutes group was demonstrated in the field by DNA extraction from the same sample, PCR amplification and fluorescent labeling of the bacterial 16S rRNA gene, and hybridization with a phylogenetic oligonucleotide microarray (Fig. 5).

Some of the antibodies raised against the Río Tinto acidic environment or acidophilic strains showed significant fluorescent signals, which indicates the presence of similar molecular biomarkers or microorganisms, or both. This is the case for peaks 1–7 in Fig. 3 (Table 3), which correspond to extracellular polymeric material or cellular fractions obtained from water, biofilms (filaments), sulfur-rich samples (dry crusts, sediments, jarosite and iron-sulfate precipitates), and peaks 8 and 9 from iron-sulfur bacteria of *Acidithiobacillus* genus. The presence of molecular biomarkers and bacteria characteristic of acidic environments might be related to the fact that Atacama soils may contain strong acids in accumulated dust particles, as reported by Quinn *et al.* (2005). They concluded that extremely low pH resulting from acid accumulation combined with limited water availability and high oxidation potential may result in acid-mediated reactions at the soil surface during low-moisture transient wetting events (*i.e.,* thin films of water). These micro-niches might support the growth of sulfur-oxidizing bacteria like *Acidithiobacillus* spp. and *Hallothiobacillus* spp., iron-reducing bacteria like *Acidocella* spp. and *Acidiphilium* spp., which may tolerate up to pH 5 (Lu *et al.,* 2010), or iron-oxidizing bacteria like *Acidimicrobium* spp.

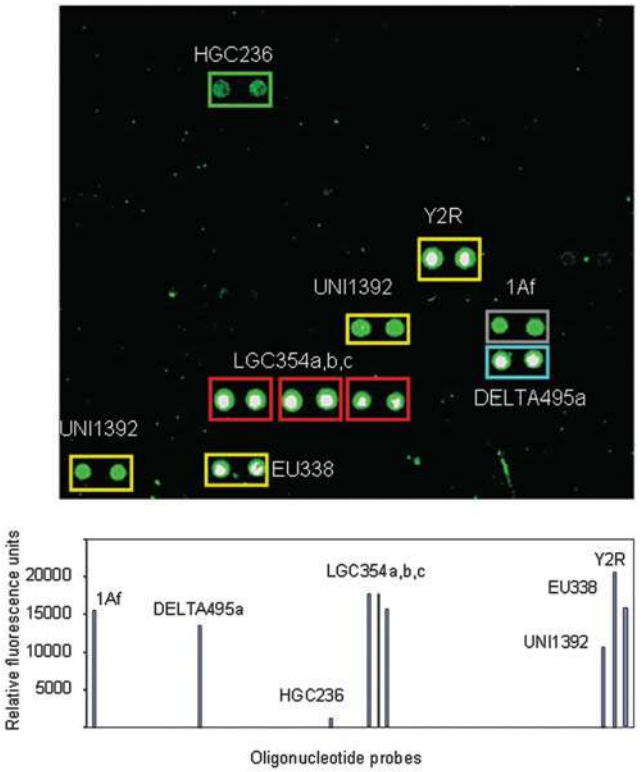

FIG. 5. Detection of bacteria by DNA hybridization in sample **200.** Microarray image showed positive fluorescent spots (*top figure*) corresponding to universal eubacterial probes (UNI1392, EU338, Y2R), high-GC-content Gram-positive bacteria (Actinomycetes group, probe HGC236), the low-GC-content Gram-positives Firmicutes including the *Lactobacillus* subgroup (LGC354a), the *Bacillus* subgroup (LGC354b), and the *Streptococcus* subgroup (LGC354c); Deltaproteobacteria (DELTA495a); and Archaea (1Af). This last probe corresponds to a highly degenerated oligonucleotide considered specific for Archaea. Because the fluorescent probe was amplified with primers for Eubacteria, we did not expect positive results with 1Af unless it came from similar sequences from unknown bacteria. (*Bottom figure*) Plot showing the quantification of fluorescent signals from nonsaturated images. Color images available online at www.liebertonline.com/ast

The relatively high fluorescent signal obtained with antibodies IVI21S1, IVJ8C1, EPS_SP raised against *Salinibacter ruber, Halorubrum* spp., and exopolymeric substances from the Santa Pola solar saltern (Alicante, Spain), respectively, indicates the presence of archaea at 2 m deep. This fact was confirmed by molecular phylogenetic studies in the laboratory by amplification and sequencing the archaeal 16S rRNA gene. Archaea have been reported in superficial samples from the Atacama (Lizama *et al.,* 2001; Demergasso *et al.,* 2004), but until very recently they were not detected in the subsurface (Gramain *et al.,* 2011). Our work further confirms and expands the presence of these prokaryotes in the Atacama soil subsurface.

Sugars and proteins followed a parallel pattern up to near 3 m, where proteins drop dramatically but sugars continue with relatively high levels. The peak in protein content could be associated with a more active microbial population, as a consequence of higher water availability due, in turn, to the presence of materials with higher deliquescence capacity. The microbial activity would produce acids that might explain the small drop in the pH of water solutions in these samples. By contrast, the permanent sugar level below 3 m might be due to the accumulation of extracellular polysaccharides (EPS) produced as a response to lower water activity, as it has been reported in some bacteria (*e.g.,* Roberson and Firestone, 1992) or in soil environments (Foster, 1981). The strong correlation between protein content, halite, small acidification, and maximal deliquescence capacity (Fig. 6) with LDChip results, together with microscopic and molecular phylogenetic analyses, indicates the presence of an actual or recently colonized habitat, a true microbial oasis.

4.2. A hygroscopic mineral-driven subsurface hypersaline habitat: implications for Mars

We described a new hypersaline subsurface habitat where the presence of hygroscopic minerals (halite, perchlorate, and anhydrite) may be responsible for water retention. Samples contained 10–41 ppm (mg Kg^{-1}) of perchlorate and a peak of NaCl of 260 g Kg^{-1} at 2 m depth, high enough to promote deliquescence. In fact, these samples showed the higher deliquescence capacity (Figs. 6 and 9) by accumulating nearly 60% of the initial weight of liquid water in 20 days (*e.g.,* sample **200**). After 5 days, no significant differences were observed; but later, a clear increase in the capacity of water absorption and deliquescence was recorded for sample **200** and those in close proximity to it, coincident with the highest halite content. Moreover, deliquescence increases when organic matter (*ca.* 1.9% in sample **200**) is removed (Fig. 10). These results are consistent with those of Davila *et al.* (2008), which demonstrated that water vapor condenses and deliquesces on the halite surface and pores at low relative humidity (75%). The ability of halite and perchlorate salts to absorb water and form a liquid solution (deliquesce) is highly relevant for the search for life on Mars. Zorzano *et al.* (2009) demonstrated that small amounts of sodium perchlorate spontaneously absorb moisture and melt into a liquid solution under martian atmospheric conditions. In addition, Davila *et al.* (2010) reported the deliquescence capacity of hygroscopic salts and their hypothetical capacity to support microbial growth or metabolic activity under simulated martian conditions.

Our AtacaMars field campaign demonstrates that subsurface hygroscopic salt environments may be true oasis for microbial life and further supports the possibility of a subsurface martian habitat based on the deliquescence capacity of similar hygroscopic salts. We hypothesize an ecosystem fueled by reduced compounds from hydrothermal activity (H_2, SH_2, acetate, formate, etc.). Potential martian microorganisms could use perchlorates, nitrates, or sulfates as electron acceptors as shown in the Atacama subsurface (Fig. 11). Strong gradients of salts can be formed, and microorganisms would use flagella to move in search of nutrients. When water is scarce, microorganisms produce abundant exopolymeric material that helps them to avoid desiccation and attaches them to mineral surfaces, where they form small biofilms or cell clusters. After the death of the microorganisms, the polymeric remains (EPS, proteins, nucleic acids, etc.) or other metabolites are retained by electrostatic charges of mineral and salt crystals. These interactions with minerals,

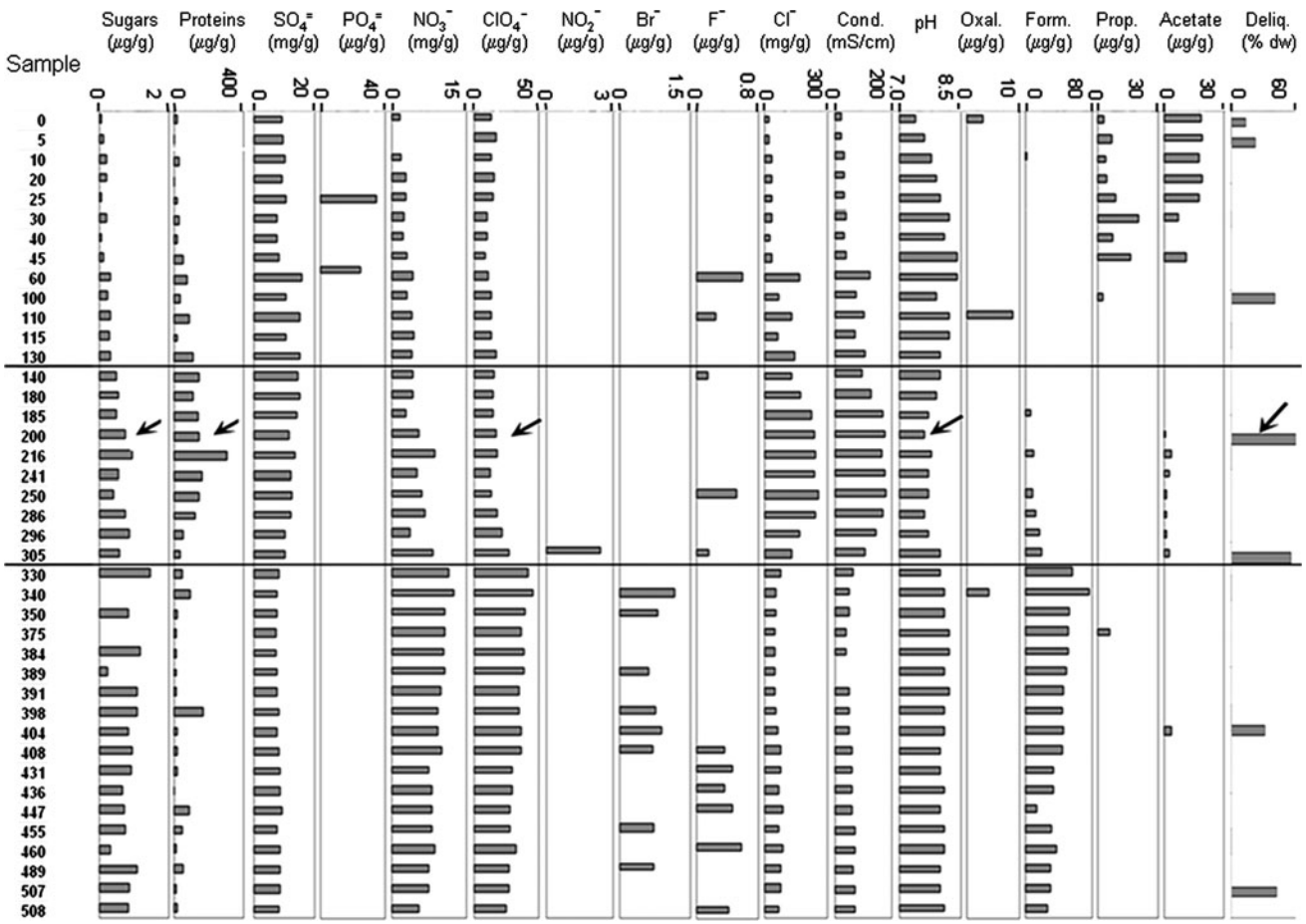

FIG. 6. Biogeochemical analyses of the samples collected along the whole core. Sample names and depths, the assayed compound or parameter, the units, and the scale are indicated at the top of the figure. Arrows point to sample **200**. The horizontal lines delimit the samples with the higher halite and protein concentration, the highest deliquescence capacity, and a small decrease in pH, defining a geological unit for a subsurface habitat. (Deliq) Deliquescence capacity of the samples after 20 days at 4°C and 75% relative humidity, expressed as the percentage (% dw) of adsorbed water with respect to the initial dry weight (2 g per sample), showing a maximum of 58% at sample **200** (See Figs. 9 and 10).

Table 4. Amino Acids Detected in Polymeric Material (>1200 Da) Extracted by Guanidine Chloride Buffer

Sample	*Amino acids*
0	Gly, Ala, +3 unidentified amines
5	Glu, Ser, Gly, Ala, +3 unidentified amines
60	Asp (traces), Glu (traces), Ser, Gly, Ala, unidentified amines
140	Asp (traces), Glu (traces), Ser, Gly, Ala, 5 unidentified amines
200	Asp, Glu, Ser, Gly, Ala, unidentified amines
286	Asp (traces), Glu (traces), Ser, Ala, Pro, Val, 2 unidentified amines
305	Asp (traces), Glu (traces), Ser, Gly, Ala, 2 unidentified amines
398	Asp, Glu, Ser, Gly, Ala, 2 unidentified amines
431	Asp (traces), Glu (traces), Ser, Gly, Thr, Ala
460	ND
507	Asp, Glu, Ser, Gly, Ala, 3 unidentified amines

ND, Not detected.

in addition to high salt concentrations, hinder enzymatic degradation. Similar niches could be present in the martian subsurface, where small organic acids can be supplied from the partial photodestruction of complex meteoritic organic matter. Halite and perchlorate salts have two main advantages to sustain a hypothetical subsurface martian ecosystem: they trap and form liquid water and simultaneously lower its freezing point. Additionally, high salt concentrations inhibit enzymes like DNAses, which allows better preservation of biological polymers.

4.3. LDChip for life detection on Mars

Our LDChip is suited to the search for microbial life in planetary exploration, particularly for Mars. We hypothesize that microorganisms living in similar habitats under similar physicochemical parameters share similar molecular mechanisms to deal with such conditions. Those mechanisms will produce similar biomolecules that constitute a good set of molecular biomarkers. We suggest two strategies for target selection: (i) a direct approach, in which well-known biomolecules or their diagenetic products from those listed by Parnell *et al.* (2007) and Parro *et al.* (2008a) are used as

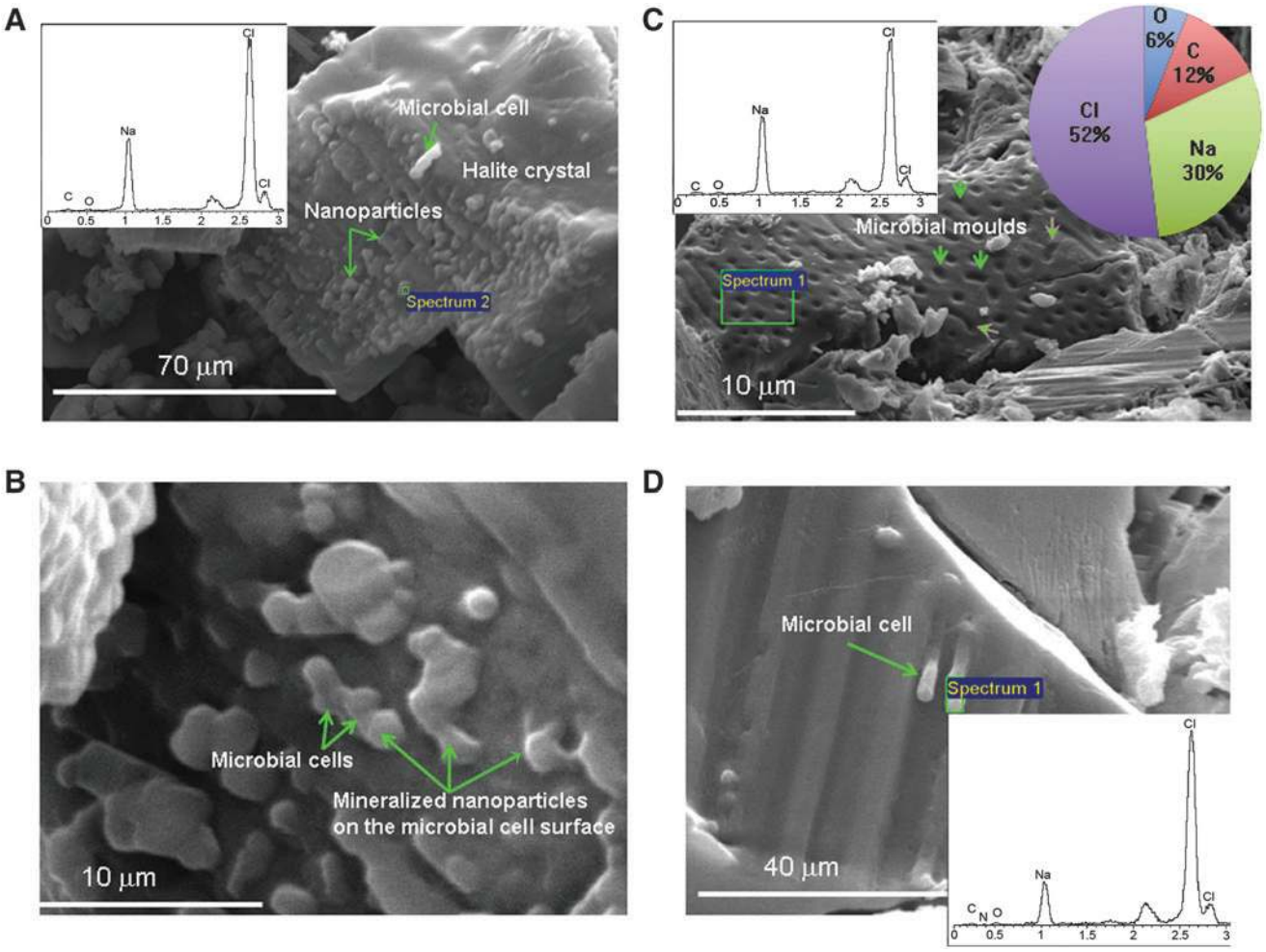

FIG. 7. Microbial forms under the Atacama surface bound to halite crystals. Scanning electron microscope images and energy dispersive X-ray (EDX) spectra showed halite crystals with incipiently mineralized microbial cells. (**A**) Halite crystal with elongated morphology and rough surface showing nanoparticles and mineralized microbial cell-like structures (arrows) on its surface. EDX spectrum of the crystal (inset) indicates that it is composed of Na and Cl (halite). (**B**) Close-up of two microbial cells from (A) attached to the halite crystal surface (arrows). (**C**) Halite crystal showing empty voids which correspond to mineralized moulds of degraded microbial cells, most probably bacteria (arrows), some of them with clear vibriod form. Note that EDX spectrum displays Na, Cl, C, O, and N. The four latter elements come, most probably, from organic compounds of microbial cells. The pie chart shows the percentage of the main elements. (**D**) Close-up of two microbial cells attached to the halite crystal surface (arrow) and the EDX spectrum of one of them. The EDX spectra correspond to the green squares. Color images available online at www.liebertonline.com/ast

antigens to produce antibodies; and (ii) a shotgun strategy where whole or fractionated biochemical extracts from terrestrial Mars analogues are used as targets for antibody production (Parro *et al.*, 2008a, 2011a; Rivas *et al.*, 2008; Parro and Muñoz-Caro 2010). We have produced polyclonal antibodies against biochemical extracts from environments that are acidic and iron-sulfur-rich, hydrothermal, permanently frozen, hypersaline, and so on (Table 2). Samples were taken from water, sediments, mineral deposits (sulfate precipitates, jarosite, hematite, etc.), rocks, and subsurface cores during drilling campaigns. Simultaneously, we can produce antibodies against different kinds of universal macromolecules like EPS, anionic polymers, cell wall components, nucleic acids, nucleotides and derivatives, phylogenetically conserved proteins, and so on. There are commercial antibodies against single- or double-stranded DNA, all recognizing structures and features of *terrestrial* DNA. In the case of an eventual martian DNA made up of slightly different nucleotides, it probably would not be recognized with antibodies against terrestrial counterparts, except in those cases where the antibodies were recognizing common structures. It is possible to make antibodies against modified nucleotides, but it is unknown which modifications to target. Alternative nucleobases (*e.g.*, xantine, aminated, or methylated derivatives of the four known nucleotides) can be used as targets. However, considering that some nucleobases (*e.g.*, adenine) can be obtained abiotically (Yuasa *et al.*, 1984), the detection of these types of compounds by itself is not a biomarker, unless they were forming part of a polymer like DNA or a secondary structure like a double or triple helix. Universal modified nucleotides that are widely used for life as signal-transducers, for example, cyclic adenosine monophosphate (cAMP) and cyclic guanosine monophosphate (cGMP) (Gomelsky, 2011), are good targets for antibody production.

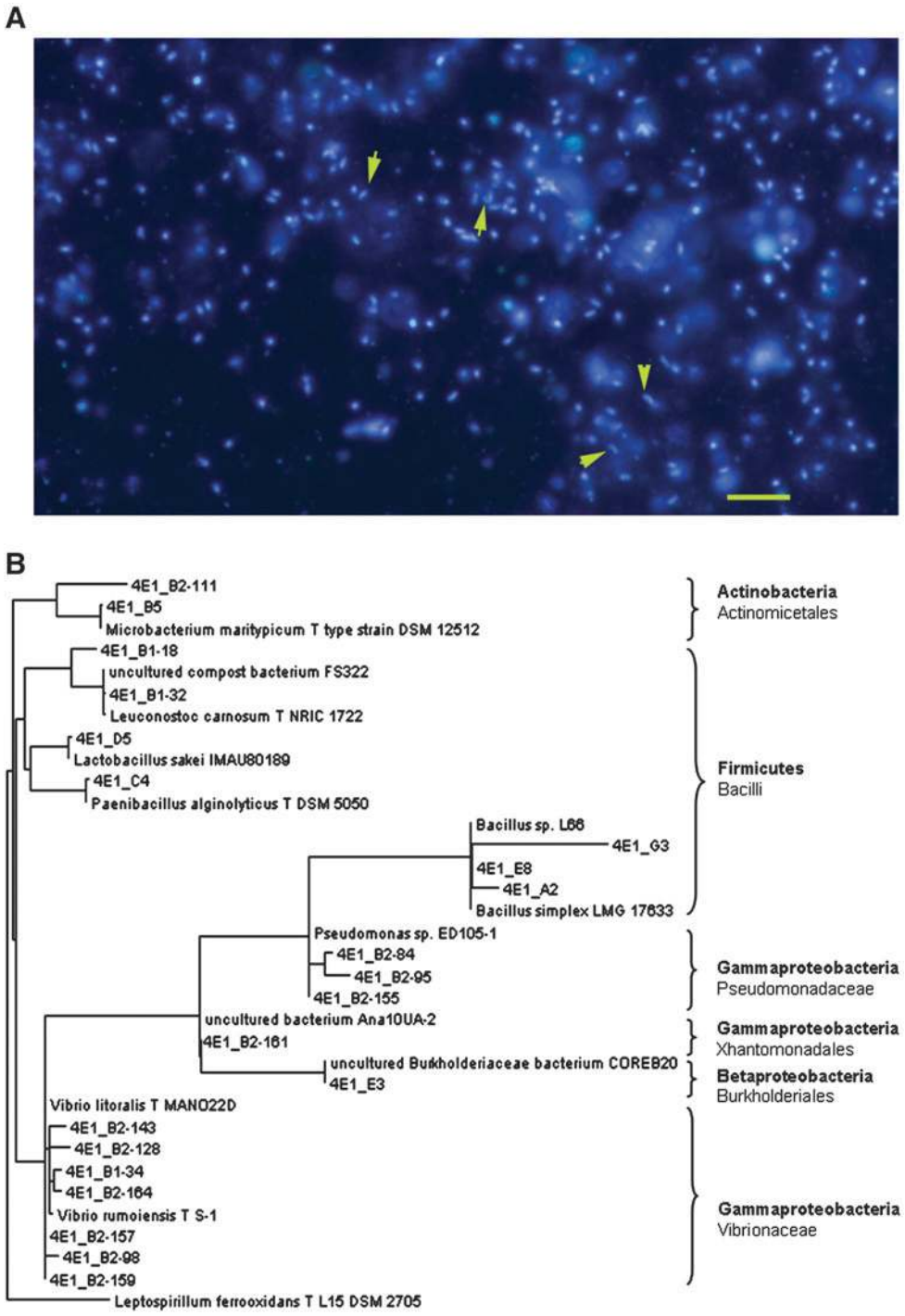

FIG. 8. Microbial cells and phylogenetic analysis of bacterial DNA from 2 m deep. (**A**) Sample **200** was stained with DNA-specific stain (DAPI). Rod- and comma-shaped or vibrioid forms (arrows) can be detected. Bar, 5 μm. (**B**) Phylogenetic tree obtained with the 16S rRNA gene sequences from sample **200** (see text for explanations). Sequences obtained from sample **200** were named as 4E1….Color images available online at www.liebertonline.com/ast

There are commercial antibodies against these compounds (Table 2), and we have also produced our own stock. In fact, LDChip300 showed strong signals for antibodies against these compounds (see peaks 46, 49, and 50, all against cGMP, in Fig. 3 and Table 3), which indicates that some microorganisms might be producing and even secreting cGMP or its derivatives. In fact, it has been recently reported that the Alphaproteobacterium *Rhodospirillum centenum* secretes relatively high amounts of cGMP to trigger the formation of metabolically dormant cells, called cysts, which are highly resistant to desiccation (Berleman and Bauer, 2004; Marden *et al.*, 2011). High salt concentration inhibits degrading enzymes, among them the nucleases, which may explain why, in this hypersaline environment, DNA and nucleotide derivatives are well-preserved. Additionally, the binding to mineral surfaces may be an additional factor of stabilization

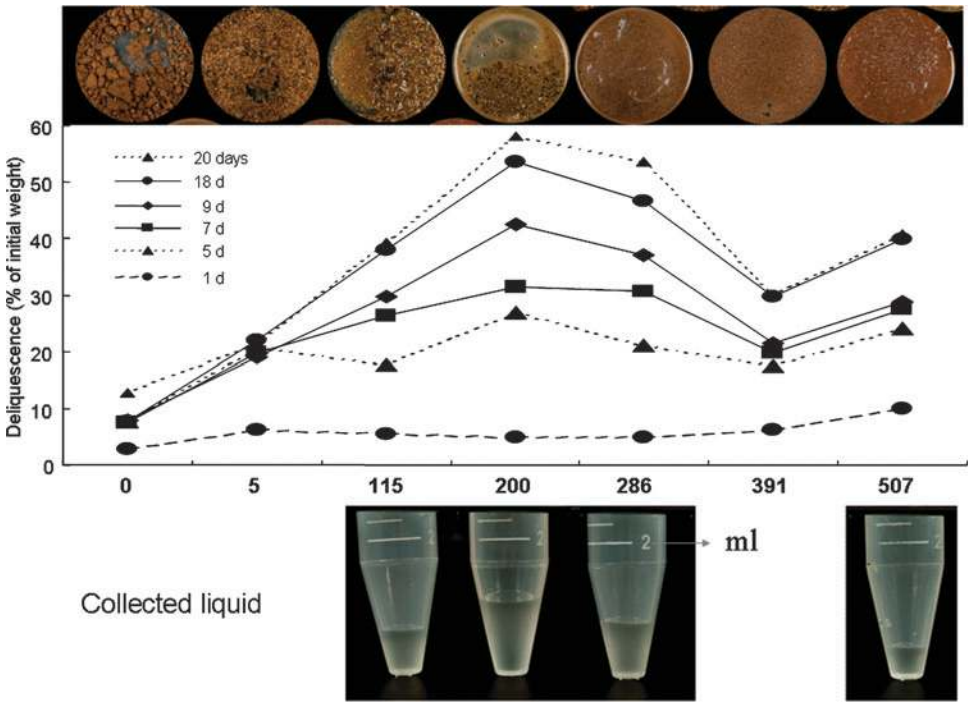

FIG. 9. Deliquescence capacity of the samples at different depths. (*Top*) Photographs showing the aspect of the samples after 20 days of deliquescence assay (see Section 2.17). The accumulation of liquid water is clearly visible. (*Middle*) The water retained by each of the samples was estimated as the percentage of the initial dry weight along the time course: 1, 5, 7, 9, 18, and 20 days. (*Bottom*) Liquid water recovered from some of the samples. Color images available online at www.liebertonline.com/ast

and aggregation (Romanowski *et al.,* 1993). Whether the positive signals obtained with anti-cGMP antibodies are indeed due to the presence of cGMP is yet to be determined. Positive signals from a SMI indicate that we are detecting at least a dimer, an oligomeric or polymeric compound, or other types of aggregate, because at least two antigen-binding sites are necessary; one to bind to the capturing antibody and another to bind to the fluorescent tracer.

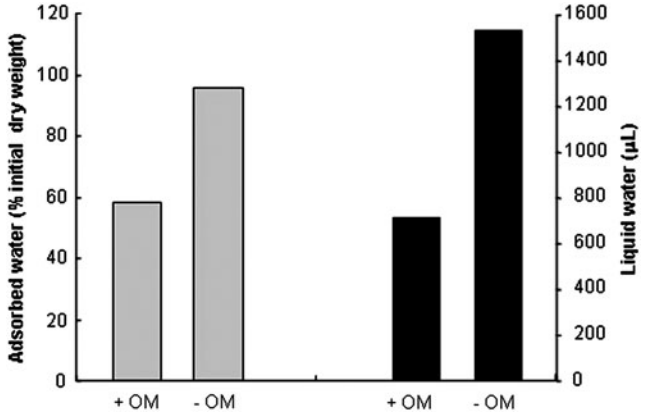

FIG. 10. The presence of *ca.* 2% organic matter in the samples diminishes the deliquescence capacity to about 50%. Two aliquots of 2 g of sample **200** were dried, their organic matter kept (+OM) or baked at 550°C to destroy it (-OM), and finally subjected to the deliquescence capacity assay for 20 days (see Materials and Methods). The adsorbed water was measured as the percentage of the initial dry weight (gray) and as the total liquid water recovered (black). Total organic carbon in sample **200** was 1.98 ± 0.15%.

LDChip300 contains antibodies against other universal compounds like protoporphyrin IX, lipidA, peptidoglycan, amino acids, vitamin K12, some antibiotics, and antibodies against proteins and peptides from relevant microbial metabolisms: nitrogen fixation; sulfate, nitrate, and perchlorate reduction; iron oxi-reduction; and so on. (Table 2). Theoretically, it is possible to produce antibodies against any type of terrestrial biomolecule or even molecules that could be considered an extraterrestrial substitute. But, given that we know only terrestrial life, we must focus on making antibodies for that.

5. Conclusion

We have discovered a new hypersaline subsurface habitat in the Atacama. The presence of highly hygroscopic salt deposits associated with the microorganisms indicates that this habitat constitutes a true microbial oasis. Hygroscopic salts promote the deliquescence of water on the mineral surfaces and form thin liquid films that can maintain microbial growth. Our LDChip300 detected microbes and molecular biomarkers in this hypersaline subsurface environment. The relatively high number of antibodies against a rational and structured panel of target molecular biomarkers makes LDChip a suitable tool for the search for life for planetary exploration. Halite- and perchlorate-rich subsurface environments on Mars should be considered targets for future life-detection missions. The known destructive effects on organic matter by thermal oxidation promoted by perchlorates (Navarro-González *et al.,* 2010) are not a constraint for our LDChip-SOLID system (Parro *et al.,* 2011a). The use of a SOLID-like Life Detector Chip and instrumentation as part of the payload of future missions could be an important contribution to the search for life on Mars.

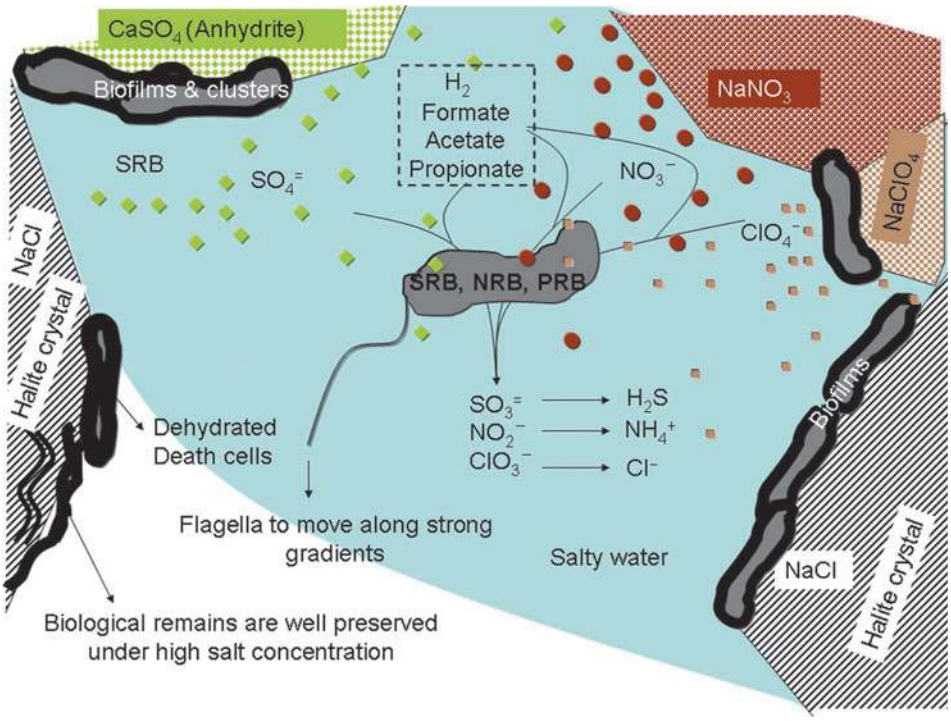

FIG. 11. A potential martian biota based on the Atacama's hypersaline subsurface habitat. Deliquescence on mineral crystals would dissolve salts and small organic compounds to provide energy sources and nutrients for microorganisms (see Section 4.2 for explanation). SRB, NRB, and PRB: sulfate-, nitrate-, and perchlorate-reducing bacteria, respectively. Color images available online at www.liebertonline.com/ast

Acknowledgments

This work has been funded by the Spanish Ministerio de Ciencia e Innovación (MICINN) grant No. AYA2008_04013. We thank Patricio Raúl Árias for his assistance in the field work, Compañía Minera Cordillera for their help during the field campaign, and Drs. Josefa Antón and Fernando Santos (Universidad de Alicante, Spain) for providing halophilic strains.

Abbreviations

BSA, bovine serum albumin; cAMP, cyclic adenosine monophosphate; EPS, exopolysaccharides; cGMP, cyclic guanosine monophosphate; LDChip, Life Detector Chip; MAAM, MultiArray Analysis Module; OTUs, operative taxonomic units; PAM, prokaryotic acidophile microarray; RDP, the Ribosomal Database Project; SAU, Sample Analysis Unit; SEM, scanning electron microscopy; SMI, sandwich microarray immunoassay; SPU, Sample Preparation Unit; SOLID, Signs Of LIfe Detector.

References

Altschul, S.F., Madden, T.L., Schäffer, A.A., Zhang, J., Zhang, Z., Miller, W., and Lipman, D.J. (1997) Gapped BLAST and PSI-BLAST: a new generation of protein database search programs. *Nucleic Acids Res* 25:3389–3402.

Berleman, J. and Bauer, C.E. (2004) Characterization of the cyst cell formation in the purple photosynthetic bacterium *Rhodospirillum centenum*. *Microbiology* 150:383–390.

Bobst, A.L., Lowenstein, T.K., Jordan, T.E., Godfrey, L.V., Ku, T.L., and Luo, S. (2001) A 106 ka paleoclimate record from drill core of the Salar de Atacama, northern Chile. *Palaeogeogr Palaeoclimatol Palaeoecol* 173:21–42.

Cabrol, N.A., Chong-Diaz, G.C., Wettergreen, D., Stoker, C.R., Dohm, J.M., Reaten, R., Schwher, K., Gulick, V.C., Landheim, R., Lee, P., Roush, T.L., Zent, A.P., Herrera-Lameli, C., Jensen Iglesia, A., Pereira Arredondo, M., Dunfield, G.C., Pedersen, L., Bualat, M.G., Christian, D., Mina, C., Sims, M.H., Thomas, H.J., Tucker, D.J., and Zbinden, E. (2001) Science results of the Atacama Nomad rover field experiment, Chile: implications for planetary exploration. *J Geophys Res* 106:7664–7675.

Cabrol, N.A., Wettergreen, D., Warren-Rhodes, K., Grin, E.A., Moersch, J., Diaz, G.C., Cockell, C.S., Coppin, P., Demergasso, C., Dohm, J.M., Ernst, L., Fisher, G., Glasgow, J., Hardgrove, C., Hock, A.N., Jonak, D., Marinangeli, L., Minkley, E., Ori, G.G., Piatek, J., Pudenz, E., Smith, T., Stubbs, K., Thomas, G., Thompson, D., Waggoner, A., Wagner, M., Weinstein, S., and Wyatt, M. (2007) Life in the Atacama: searching for life with rovers (science overview). *J Geophys Res* 112, doi:10.1029/2006JG000298.

Cameron, R. (1969) Abundance of microflora in soils of desert regions. NASA Technical Report 32-1378, National Aeronautics and Space Administration, Washington DC.

Chong-Díaz, G., Mendoza, M.N., García-Veigas, J., Pueyo, J.J., and Turner, P. (1999) Evolution and geochemical signatures in a Neogene forearc evaporitic basin: the Salar Grande (Central Andes of Chile). *Palaeogeogr Palaeoclimatol Palaeoecol* 151:39–54.

Cole, J.R., Wang, Q., Cardenas, E., Fish, J., Chai, B., Farris, R.J., Kulam-Syed-Mohideen, A.S., McGarrell, D.M., Marsh, T., Garrity, G.M., and Tiedje, J.M. (2009) The Ribosomal Database Project: improved alignments and new tools for rRNA analysis. *Nucleic Acids Res* 37:D141–D145.

Dartnell, L.R., Desorgher, L., Ward, J.M., and Coates, A.J. (2007) Modeling the surface and subsurface martian radiation environment: implications for astrobiology. *Geophys Res Lett* 34, doi:10.1029/2006GL027494.

Davila, A.F., Gómez-Silva, B., de los Rios, A., Ascaso, C., Olivares, H., McKay, C.P., and Wierzchos, J. (2008) Facilitation of endolithic microbial survival in the hyperarid core of the Atacama Desert by mineral deliquescence. *J Geophys Res* 113, doi:10.1029/2007JG000561.

Davila, A.F., Duport, L.G., Melchiorri, R., Jänchen, J., Valea, S., de Los Rios, A., Fiaren, A.G., Möhlmann, D., McKay, C.P., Ascaso, C., and Wierzchos, J. (2010) Hygroscopic salts and the potential for life on Mars. *Astrobiology* 10:617–628.

Delong, E.F. (1992) Archaea in coastal marine environments. *Proc Natl Acad Sci USA* 89:5685–5689.

Demergasso, C., Casamayor, E.O., Chong, G., Galleguillos, P., Escudero, L., and Pedrós-Alió, C. (2004) Distribution of prokaryotic genetic diversity in athalassohaline lakes of the Atacama Desert, Northern Chile. *FEMS Microbiol Ecol* 48:57–69.

Dubois, M., Gilles, K.A., Hamilton, J.K., Rebers, P.A., and Smith, F. (1956) Colorimetric method for determination of sugars and related substances. *Anal Chem* 28:350–356.

Ewing, B., Hillier, L., Wendl, M., and Green, P. (1998) Base-calling of automated sequencer traces using phred I Accuracy assessment. *Genome Res* 8:175–185.

Fernández-Calvo, P., Näke, C., Rivas, L.A., García-Villadangos, M., Gómez-Elvira, J., and Parro, V. (2006) A multi-array competitive immunoassay for the detection of broad range molecular size organic compounds relevant for astrobiology. *Planet Space Sci* 54:1612–1621.

Fish, S.A., Shepherd, T.J., McGenity, T.J., and Grant, W.D. (2002) Recovery of 16S ribosomal RNA gene fragments from ancient halite. *Nature* 417:432–436.

Foster, R.C. (1981) Polysaccharides in soil fabrics. *Science* 214:665–667.

Garrido, P., González-Toril, E., García-Moyano, A., Moreno-Paz, M., Amils, R., and Parro, V. (2008) An oligonucleotide prokaryotic acidophile microarray (PAM): its validation and its use to monitor seasonal variations in extreme acidophilic environments with total environmental RNA. *Environ Microbiol* 10:836–850.

Glavin, D.P., Cleaves, H.J., Schubert, M., Aubrey, A., and Bada, J.L. (2004) New method for estimating bacterial cell abundances in natural samples by use of sublimation. *Appl Environ Microbiol* 70:5923–5928.

Gomelsky, M. (2011) cAMP, c-di-GMP, c-di-AMP and now cGMP: bacteria use them all! *Mol Microbiol* 79:562–565.

Gordon, D. (2004) Viewing and editing assembled sequences using Consed. In *Current Protocols in Bioinformatics,* edited by A.D. Baxevanis and D.B. Davison, John Wiley & Sons, New York, pp 11.2.1–11.2.43.

Gramain, A., Díaz, G.C., Demergasso, C., Lowenstein, T.K., and McGenity, T.J. (2011) Archaeal diversity along a subterranean salt core from the Salar Grande (Chile). *Environ Microbiol* 13:2105–2121.

Hecht, M.H., Kounaves, S.P., Quinn, R.C., West, S.J., Young, S.M., Ming, D.W., Catling, D.C., Clark, B.C., Boynton, W.V., Hoffman, J., Deflores, L.P., Gospodinova, K., Kapit, J., and Smith, P.H. (2009) Detection of perchlorate and the soluble chemistry of martian soil at the Phoenix lander site. *Science* 325:64–67.

Huber, T., Faulkner, G., and Hugenholtz, P. (2004) Bellerophon; a program to detect chimeric sequences in multiple sequence alignments. *Bioinformatics* 20:2317–2319.

Kminek, G. and Bada, J.L. (2006) The effect of ionizing radiation on the preservation of amino acids on Mars. *Earth Planet Sci Lett* 245:1–15.

Lizama, C., Monteoliva-Sánchez, M., Prado, B., Ramos-Cormenzana, A., Weckesser, J., and Campos, V. (2001) Taxonomic study of extreme halophilic archaea isolated from the "Salar de Atacama", Chile. *Syst Appl Microbiol* 24:464–474.

Lester, E.D., Satomi, M., and Ponce, A. (2007) Microflora of extreme arid Atacama Desert soils. Soil Biol Biochem 39:704–708.

Lu, S., Gischkat, S., Reiche, M., Akob, D.M., Hallberg, K.B., and Küsel, K. (2010) Ecophysiology of Fe-cycling bacteria in acidic sediments. *Appl Environ Microbiol* 76:8174–8183.

Marden, J.N., Dong, Q., Roychowdhury, S., Berleman, J.E., and Bauer, C.E. (2011) Cyclic GMP controls *Rhodospirillum centenum* cyst development. *Mol Microbiol* 79:600–615.

McLennan, S.M., Bell, J.F., III, Calvin, W.M., Christensen, P.R., Clark, B.C., de Souza, P.A., Farmer, J., Farrand, W.H., Fike, D.A., Gellert, R., Ghosh, A., Glotch, T.D., Grotzinger, J.P., Hahn, B., Herkenhoff, K.E., Hurowitz, J.A., Johnson, J.R., Johnson, S.S., Jolliff, B., Klingelhöfer, G., Knoll, A.H., Learner, Z., Malin, M.C., McSween, H.Y., Pocock, J., Ruff, S.W., Soderblom, L.A., Squyres, S.W., Tosca, N.J., Watters, W.A., Wyatt, M.B., and Yen, A. (2005) Provenance and diagenesis of the evaporite-bearing Burns Formation Meridiani Planum Mars. *Earth Planet Sci Lett* 240:95–121.

Murchie, S.L., Mustard, J.F., Ehlmann, B.L., Miliken, R.E., Bishop, J.L., McKeown, N.K., Dobrea, E.Z.N., Seelos, F.P., Buczkowski, D.L., Wiseman, S.M., Arvidson, R.E., Wray, J.J., Swayze, G., Clark, R.N., Des Marais, D.J., McEwen, A.S., and Bibring, J.P. (2009) A synthesis of martian aqueous mineralogy after 1 Mars year of observations from the Mars Reconnaissance Orbiter. *J Geophys Res* 114, doi:10.1029/2009JE003342.

Navarro-González, R., Rainey, F.A., Molina, P., Bagaley, D.R., Hollen, B.J., de la Rosa, J., Small, A.M., Quinn, R.C., Grunthaner, F.J., Cáceres, L., Gómez-Silva, B., and McKay, C.P. (2003) Mars-like soils in the Atacama Desert, Chile, and the dry limit of microbial life. *Science* 302:1018–1021.

Navarro-González, R., Vargas, E., de la Rosa, J., Raga, A.C., and McKay, C.P. (2010) Reanalysis of the Viking results suggests perchlorate and organics at mid-latitudes on Mars. *J Geophys Res* 115, doi:10.1029/2010JE003599.

Osterloo, M.M., Hamilton, V.E., Bandfield, J.L., Glotch, T.D., Baldridge, A.M., Christensen, P.R., Tornabene, L.L., and Anderson, F.S. (2008) Chloride-Bearing Materials in the Southern Highlands of Mars. *Science* 319:1651–1654.

Parnell, J., Cullen, D., Sims, M.R., Bowden, S., Cockell, C.S., Court, R., Ehrenfreund, P., Gaubert, F., Grant, W., Parro, V., Rohmer, M., Sephton, M., Stan-Lotter, H., Steele, A., Toporski, J., and Vago, J. (2007) Searching for life on Mars: selection of molecular targets for ESA's Aurora ExoMars mission. *Astrobiology* 7:578–604.

Parro, V. (2010) Antibody microarrays for environmental monitoring. In *Handbook of Hydrocarbon and Lipid Microbiology,* edited by K.N. Timmis, Springer-Verlag Berlin, pp 2699–2710.

Parro, V. and Muñoz-Caro, G. (2010) Solid carbonaceous and organic matter in space, macromolecular complexes, biomarkers, and microarray-based instrumentation for *in situ* detection. In *Astrobiology: Emergence, Search and Detection of Life,* edited by V.A. Basiuk, American Scientific Publishers, Los Angeles, pp 376–398.

Parro, V., Rodríguez-Manfredi, J.A., Briones, C., Compostizo, C., Herrero, P.L., Vez, E., Sebastián, E., Moreno-Paz, M., García-Villadangos, M., Fernández-Calvo, P., González-Toril, E., Pérez-Mercader, J., Fernández-Remolar, D., and Gómez-Elvira, J. (2005) Instrument development to search for biomarkers on mars: terrestrial acidophile iron-powered chemolithoautotrophic communities as model systems. *Planet Space Sci* 53:729–737.

Parro, V., Rivas, L.A., and Gómez-Elvira J. (2008a) Protein microarrays-based strategies for life detection in astrobiology. *Space Sci Rev* 135:293–311.

Parro, V., Fernández-Calvo, P., Rodríguez Manfredi, J.A., Moreno-Paz, M., Rivas, L.A., García-Villadangos, M., Bonaccorsi, R., González-Pastor, J.E., Prieto-Ballesteros, O., Schuerger, A.C., Davidson, M., Gómez-Elvira, J., and Stoker, C.R. (2008b) SOLID2: an antibody array-based life-detector instrument in a Mars drilling simulation experiment (MARTE). *Astrobiology* 8:987–999.

Parro, V., de Diego-Castilla, G., Rodríguez-Manfredi, J.A., Rivas, L.A., Blanco-López, Y., Sebastián, E., Romeral, J., Compostizo, C., Herrero, P.L., García-Marín, A., Moreno-Paz, M., García-Villadangos, M., Cruz-Gil, P., Peinado, V., Martín-Soler, J., Pérez-Mercader, J., and Gómez-Elvira, J. (2011a) SOLID3: a multiplex antibody microarray-based optical sensor instrument for *in situ* life detection in planetary exploration. *Astrobiology* 11:15–28.

Parro, V., Fernández-Remolar, D., Rodríguez-Manfredi, J.A., Cruz-Gil, P., Rivas, L.A., Ruiz-Bermejo, M., Moreno-Paz, M., García-Villadangos, M., Gómez-Ortiz, D., Blanco-López, Y., Menor-Salván, C., Prieto-Ballesteros, O., and Gómez-Elvira, J. (2011b) Classification of modern and old Río Tinto sedimentary deposits through the biomolecular record using a life marker biochip: implications for detecting life on Mars. *Astrobiology* 11:29–44.

Piatek, J.L., Hardgrove, C., Moersch, J.E., Drake, D.M., Wyatt, M.B., Rampey, M., Carlisle, O., Warren-Rhodes, K., Dohm, J.M., Hock, A.N., Carbol, N.A., Wettergreen, D.S., Grin, E.A., Diaz, G.C., Coppin, P., Weinstein, S., Cockell, C.S., Marinangeli, L., Ori, G.G., Smith, T., Jonak, D., Wagner, M., Stubbs, K., Thomas, G., Pudenz, E., and Glasgow, J. (2007) Surface and subsurface composition of the life in the Atacama field sites from rover data and orbital image analysis. *J Geophys Res* 112, doi:10.1029/2006JG000317.

Quinn, R.C., Zent, A.P., Grunthaner, F.J., Ehrenfreund, P., Taylor, C.L., and Garry, J.R.C. (2005) Detection and characterization of oxidizing acids in the Atacama Desert using the Mars Oxidation Instrument. *Planet Space Sci* 53:1376–1388.

Rivas, L.A., García-Villadangos, M., Moreno-Paz, M., Cruz-Gil, P., Gómez-Elvira, J., and Parro, V. (2008) A 200-antibody microarray biochip for environmental monitoring: searching for universal microbial biomarkers through immunoprofiling. *Anal Chem* 80:7970–7979.

Rivas, L.A, Aguirre, J., Blanco, Y., González-Toril, E., and Parro V. (2011) Graph-based deconvolution analysis of multiplex sandwich microarray immunoassays: applications for environmental monitoring. *Environ Microbiol* 13:1421–1432.

Roberson, E.B. and Firestone, M.K. (1992) Relationship between desiccation and exopolysaccharide production in a soil *Pseudomonas* sp. *Appl Environ Microbiol* 58:1284–1291.

Romanowski, G., Lorenz, M.G., and Wackernagel, W. (1993) Plasmid DNA in a groundwater aquifer microcosm-adsorption, DNAase resistance and natural genetic transformation of *Bacillus subtilis*. *Mol Ecol* 2:171–181.

Ruiz-Bermejo, M., Menor-Salván, C., Osuna-Esteban, S., and Veintemillas-Verdaguer, S. (2007) Prebiotic microreactors: a synthesis of purines and dihydroxy compounds in aqueous aerosol. *Orig Life Evol Biosph* 37:123–142.

Schloss, P.D., Westcott, S.L., Ryabin, T., Hall, J.R., Hartmann, M., Hollister, E.B., Lesniewski, R.A., Oakley, B.B., Parks, D.H., Robinson, C.J., Sahl, J.W., Stres, B., Thallinger, G.G., Van Horn, D.J., and Weber, C.F. (2009) Introducing mothur: open-source platform-independent community-supported software for describing and comparing microbial communities. *Appl Environ Microbiol* 75:7537–7541.

Schweitzer, M.H., Wittmeyer, J., Avci, R., and Pincus, S. (2005) Experimental support for an immunological approach to the search for life on other planets. *Astrobiology* 5:30–47.

Shafaat, H.S., Cable, M.L., Ikeda, M.K., Kirby, J.P., Pelletier, C.C., and Ponce, A. (2005) Towards an *in situ* endospore detection instrument. In *Proceedings of the IEEE Aerospace Conference,* Institute of Electrical and Electronics Engineers (IEEE), New York, pp 660–669.

Shkrob, I.A., Chemerisov, S.D., and Marin, T.W. (2010) Photocatalytic decomposition of carboxylated molecules on light-exposed martian regolith and its relation to methane production on Mars. *Astrobiology* 10:425–436.

Skelley, A.M., Scherer, J.R., Aubrey, A.D., Grover, W.H., Ivester, R.H.C., Ehrenfreund, P., Grunthaner, F.J., Bada, J.L., and Mathies, R.A. (2005). Development and evaluation of a microdevice for amino acid biomarker detection and analysis on Mars. *Proc Natl Acad Sci USA* 102:1041–1046.

Smith, P.K., Krohn, R.I., Hermanson, G.T., Mallia, A.K., Gartner, F.H., Provenzano, M.D., Fujimoto, E.K., Goeke, N.M., Olson, B.J., and Klenk, D.C. (1985) Measurement of protein using bicinchoninic acid. *Anal Biochem* 150:76–85.

Stahl, D.A. and Amann, R. (1991) Development and application of nucleic acid probes. In *Nucleic Acid Techniques in Bacterial Systematics,* edited by E. Stackebrandt and M. Goodfellow, John Wiley & Sons, Chichester, UK, pp 205–248.

Stan-Lotter, H., Leuko, S., Legat, A., Fendrihan, S. (2006) The assessment of the viability of halophilic microorganisms in natural communities. In *Methods in Microbiology. Extremophiles,* edited by A. Oren and F. Rainey, Elsevier, Oxford, pp 569–584.

Tuross, N. and Stathoplos, L. (1993) Ancient proteins in fossil bones. *Methods Enzymol* 224:121–129.

Weete, J.D., Abril, M., and Blackwell, M. (2010) Phylogenetic distribution of fungal sterols. *PLoS One* 5:e10899.

Weinstein, S., Pane, D., Ernst L.A., Warren-Rhodes, K., Dohm, J.M., Hock, A.N., Piatek, J.L., Emani, S., Lanni, F., Wagner, M., Fisher, G.W., Minkley, E., Dansey, L.E., Smith, T., Grin, E.A., Stubbs, K., Thomas, G., Cockell, C.S., Marinangeli, L., Ori, G.G., Heys, S., Teza, J.P., Moersch, J.E., Coppin, P., Diaz, G.C., Wettergreen, D.S., Cabrol, N.A., and Waggoner, A.S. (2008) Application of pulsed-excitation flourescence imager for daylight detection of sparse life in tests in the Atacama Desert. *J Geophys Res* 113, doi:10.1029/2006JG000319.

Yuasa, S., Flory, D., Basile, B., and Oró, J. (1984) Abiotic synthesis of purines and other heterocyclic compounds by the action of electrical discharges. *J Mol Evol* 21:76–80.

Zorzano, M.P., Mateo-Martí, E., Prieto-Ballesteros, O., Osuna, S., and Renno, N. (2009) Stability of liquid saline water on present day Mars. *Geophys Res Lett* 36, doi:10.1029/2009GL040315.

Address correspondence to:
Víctor Parro
Department of Molecular Evolution
Centro de Astrobiología (INTA-CSIC)
Carretera de Ajalvir km 4
Torrejón de Ardoz, 28850
Madrid
Spain

E-mail: parrogv@inta.es

Submitted 23 March 2011
Accepted 1 September 2011

(*Table 2 in Appendix follows* →)

Appendix

Table 2. Antibodies Developed and Used in This Work

Ab No	*Ab name*	*Source/Strain*	*Sample/Culture conditions*	*Immunogen/Fraction*	*Host*	*Supp. References*
1	IA1C1	Río Tinto (3.2 water dam)	Water	Cellular fraction	Rb	Rivas *et al.*, 2008
2	IA1S1	Río Tinto (3.2 water dam)	Water	Supernatant	Rb	Rivas *et al.*, 2008
3	IA1S2	Río Tinto (3.2 water dam)	Water	Supernatant from EDTA wash	Rb	Rivas *et al.*, 2008
4	IA1C2	Río Tinto (3.2 water dam)	Water	Insoluble cell pellet from S100	Rb	Rivas *et al.*, 2008
5	IA1S100	Río Tinto (3.2 water dam)	Water	Soluble cellular fraction S100	Rb	Rivas *et al.*, 2008
6	IA1C3	Río Tinto (3.2 water dam)	Water	EDTA washed cells (sonicated)	Rb	Rivas *et al.*, 2008
7	IA2C1	Río Tinto (3.1 stream)	Green filaments	Cellular fraction	Rb	Rivas *et al.*, 2008
8	IA2S1	Río Tinto (3.1 stream)	Green filaments	Supernatant	Rb	Rivas *et al.*, 2008
9	IA3C1	Río Tinto (3.1 stream)	Black filaments	Cellular fraction	Rb	Rivas *et al.*, 2008
10	IA3S1	Río Tinto (3.1 stream)	Black filaments	Supernatant	Rb	Rivas *et al.*, 2008
11	IC1C1	Río Tinto (Playa 3.2)	Sediments	Cellular fraction	Rb	Rivas *et al.*, 2008
12	IC1S1	Río Tinto (Playa 3.2)	Sediments	Supernatant	Rb	Rivas *et al.*, 2008
13	IC1S2	Río Tinto (Playa 3.2)	Sediments	Supernatant from EDTA wash	Rb	Rivas *et al.*, 2008
14	IC2C1	Río Tinto (3.1 water dam)	Dark red sediments	Cellular fraction	Rb	Rivas *et al.*, 2008
15	IC2S2	Río Tinto (3.1 water dam)	Dark red sediments	Supernatant from EDTA wash	Rb	Rivas *et al.*, 2008
16	IC2C3	Río Tinto (3.1 water dam)	Dark red sediments	EDTA washed cells (sonicated)	Rb	Rivas *et al.*, 2008
17	IC3C1	Río Tinto (Main spring)	Brown filaments	Cellular fraction	Rb	Rivas *et al.*, 2008
18	IC3S2	Río Tinto (Main spring)	Brown filaments	Supernatant from EDTA wash	Rb	Rivas *et al.*, 2008
19	IC3C3	Río Tinto (Main spring)	Brown filaments	EDTA washed cells (sonicated)	Rb	Rivas *et al.*, 2008
20	IC4C1	Río Tinto (3.2 water dam)	Brown filaments	Cellular fraction	Rb	Rivas *et al.*, 2008
21	IC4S2	Río Tinto (3.2 water dam)	Brown filaments	Supernatant from EDTA wash	Rb	Rivas *et al.*, 2008
22	IC5C1	Río Tinto (Playa 3.1)	Red crusts	Cellular fraction	Rb	Rivas *et al.*, 2008
23	IC5S1	Río Tinto (Playa 3.1)	Red crusts	Supernatant	Rb	Rivas *et al.*, 2008
24	IC6C1	Río Tinto (Playa 3.1)	Red sediment 1–2 cm under crust	Cellular fraction	Rb	Rivas *et al.*, 2008
25	IC6S1	Río Tinto (Playa 3.1)	Red sediment 1–2 cm under crust	Supernatant	Rb	Rivas *et al.*, 2008
26	IC7C1	Río Tinto (3.2 water dam)	Dried wall sediments	Cellular fraction	Rb	Rivas *et al.*, 2008
27	IC8C1	Río Tinto (3.1 stream's banks)	Green-orange sediments	Cellular fraction	Rb	Rivas *et al.*, 2008
28	IC8S1	Río Tinto (3.1 stream's banks)	Green-orange sediments	Supernatant	Rb	Rivas *et al.*, 2008
29	IC9C1	Río Tinto (3.1 mine's ruins)	Red-grey sulfate-rich precipitates	Cellular fraction	Rb	Rivas *et al.*, 2008
30	A138	Río Tinto ("Nacimiento")	Yellow mats (central stream)	Whole Gu/HCl extraction	Rb	Rivas *et al.*, 2008
31	A140	Río Tinto (3.0 stream)	Pink superficial layer	Cellular fraction	Rb	Rivas *et al.*, 2008
32	A141	Río Tinto (3.0 stream)	Pink superficial layer	Supernatant	Rb	Rivas *et al.*, 2008
33	A143	Río Tinto (3.2 water dam)	Wall sediments. Lithified overgrowth	Whole Gu/HCl extraction	Rb	Rivas *et al.*, 2008
34	A152	Río Tinto (3.0 stream)	Pink superficial layer	Whole Gu/HCl extraction	Rb	Rivas *et al.*, 2008
35	ID1C1	Río Tinto (Main spring)	Iron sulfate–rich precipitates	Cellular fraction	Rb	Rivas *et al.*, 2008
36	ID1S1	Río Tinto (Main spring)	Iron sulfate–rich precipitates	Supernatant	Rb	Rivas *et al.*, 2008
37	ID1S2	Río Tinto (Main spring)	Iron sulfate–rich precipitates	Supernatant from EDTA wash	Rb	Rivas *et al.*, 2008
38	ID1C3	Río Tinto (Main spring)	Iron sulfate–rich precipitates	EDTA washed cells (sonicated)	Rb	Rivas *et al.*, 2008
39	ID2S2	Peña de Hierro (148 m deep)	4-59c sample (MARTE project)	Supernatant from EDTA wash	Rb	Rivas *et al.*, 2008
40	ID3S2	Peña de Hierro (96 m deep)	4-39c sample (MARTE project)	Supernatant from EDTA wash	Rb	Rivas *et al.*, 2008
41	ID4S2	Peña de Hierro (154 m deep)	4-61a sample (MARTE project)	Supernatant from EDTA wash	Rb	Rivas *et al.*, 2008
42	ID5S2	Peña de Hierro (141 m deep)	4-56c sample (MARTE project)	Supernatant from EDTA wash	Rb	Rivas *et al.*, 2008

(*continued*)

Table 2. (Continued)

Ab No	Ab name	Source/Strain	Sample/Culture conditions	Immunogen/Fraction	Host	Supp. References
43	ID7S2	Peña de Hierro (84–97 m deep)	8-42b+43c+45abc+46bc (MARTE project)	Supernatant from EDTA/guanidinium	Rb	Rivas *et al.*, 2008
44	ID10S2	Peña de Hierro (119–127 m deep)	8-54a+54c+56c (MARTE project)	Supernatant from EDTA/guanidinium	Rb	Rivas *et al.*, 2008
45	ID11S2	Peña de Hierro (138 m deep)	8-60b+60c (MARTE project)	Supernatant from EDTA/guanidinium	Rb	Rivas *et al.*, 2008
46	ID12S2	Peña de Hierro (147–152 m deep)	8-63b+64b+64c+65b (MARTE project)	Supernatant from EDTA/guanidinium	Rb	Rivas *et al.*, 2008
47	ID13S2	Peña de Hierro (2–3 m deep)	8-2a (MARTE project)	Supernatant from EDTA/guanidinium	Rb	Rivas *et al.*, 2008
48	ID18S2	Peña de Hierro (93 m deep)	8-45b (MARTE project)	Supernatant from EDTA/guanidinium	Rb	Rivas *et al.*, 2008
49	ID14S2	Peña de Hierro (105 m deep)	8-49b (MARTE project)	Supernatant from EDTA/guanidinium	Rb	Rivas *et al.*, 2008
50	ID15S2	Peña de Hierro (119 m deep)	8-54a (MARTE project)	Supernatant from EDTA/guanidinium	Rb	Rivas *et al.*, 2008
51	ID16S2	Peña de Hierro (152 m deep)	8-65b (MARTE project)	Supernatant from EDTA/guanidinium	Rb	Rivas *et al.*, 2008
52	ID17C1	Río Tinto (3.2 water dam)	Yellow Fe-S–rich salt precipitates	Cellular fraction	Rb	Rivas *et al.*, 2008
53	ID17S1	Río Tinto (3.2 water dam)	Yellow Fe-S–rich salt precipitates	Supernatant	Rb	Rivas *et al.*, 2008
54	Ahyd	Yellowstone National Park	*Hydrogenobacter acidophilus* (Bacteria, Aquificae)	Whole cells	Rb	Schweitzer *et al.*, 2005
55	Acyan	Yellowstone National Park	*Cyanidium* spp. (Eukaryote, Rhodophyta)	Whole cells	Rb	Schweitzer *et al.*, 2005
56	A185	*Acidiphilium* spp.	Batch culture	Whole cells (intact + sonicated)	Rb	Parro *et al.*, 2005
57	A139	*Leptospirillum ferrooxidans*	Batch (N_2 fixing)	Sonicated cells	Rb	Parro *et al.*, 2005
58	A186	*L. ferrooxidans*	Batch culture	Whole cells (intact + sonicated)	Rb	Parro *et al.*, 2005
59	IVE1C1	*L. pherrifilum* (LPH2)	Fermentor	Whole cells	Rb	Rivas *et al.*, 2008
60	IVE1S1	*L. pherrifilum* (LPH2)	Fermentor	Culture supernatant	Rb	Rivas *et al.*, 2008
61	IVE1C2	*L. pherrifilum* (LPH2)	Fermentor	Insoluble cell pellet from S100	Rb	Rivas *et al.*, 2008
62	IVE1S100	*L. pherrifilum* (LPH2)	Fermentor	Soluble cellular fraction S100	Rb	Rivas *et al.*, 2008
63	IVE1BF	*L. pherrifilum* (LPH2)	Fermentor	Biofilm	Rb	Rivas *et al.*, 2008
64	IVE2C1	*L. pherrifilum* spp.	Batch + Fe^{2+}	Whole cells	Rb	Rivas *et al.*, 2008
65	IVE2S1	*L. pherrifilum* spp.	Batch + Fe^{2+}	Culture supernatant	Rb	Rivas *et al.*, 2008
66	IVE2S100	*L. pherrifilum* spp.	Batch + Fe^{2+}	Soluble cellular fraction S100	Rb	Rivas *et al.*, 2008
67	A182	*Acidithiobacillus ferrooxidans*	Batch + Fe^{2+}	Whole cells	Rb	Parro *et al.*, 2005
68	A183	*At. ferrooxidans*	Batch + Fe^{2+}	Whole cells (sonicated)	Rb	Parro *et al.*, 2005
69	IVE3C1	*At. ferrooxidans*	Batch + Fe^{2+}	Whole cells	Rb	Rivas *et al.*, 2008
70	IVE3S1	*At. ferrooxidans*	Batch + Fe^{2+}	Culture supernatant	Rb	Rivas *et al.*, 2008
71	IVE3C2	*At. ferrooxidans*	Batch + Fe^{2+}	Insoluble cell pellet from S100	Rb	Rivas *et al.*, 2008
72	IVE3S100	*At. ferrooxidans*	Batch + Fe^{2+}	Soluble cellular fraction S100	Rb	Rivas *et al.*, 2008
73	A184	*At. thiooxidans*	Batch + S	Whole cells (intact + sonicated)	Rb	Parro *et al.*, 2005
74	IVE4C1	*At. thiooxidans*	Batch + S	Whole cells	Rb	Rivas *et al.*, 2008
75	IVE4C2	*At. thiooxidans*	Batch + S	Insoluble cell pellet from S100	Rb	Rivas *et al.*, 2008
76	IVE4S100	*At. thiooxidans*	Batch + S	Soluble cellular fraction S100	Rb	Rivas *et al.*, 2008

(*continued*)

Table 2. (Continued)

Ab No	Ab name	Source/Strain	Sample/Culture conditions	Immunogen/Fraction	Host	Supp. References
77	IVE5C1	*At. albertensis*	Batch+S	Whole cells	Rb	Rivas *et al.*, 2008
78	IVE5C2	*At. albertensis*	Batch+S	Insoluble cell pellet from S100	Rb	Rivas *et al.*, 2008
79	IVE5S100	*At. albertensis*	Batch+S	Soluble cellular fraction S100	Rb	Rivas *et al.*, 2008
80	IVE6C1	*At. caldus*	Batch+S	Whole cells	Rb	Rivas *et al.*, 2008
81	IVE6S2	*At. caldus*	Batch+S	Supernatant from EDTA wash	Rb	Rivas *et al.*, 2008
82	IVE6C2	*At. caldus*	Batch+S	Insoluble cell pellet from S100	Rb	Rivas *et al.*, 2008
83	IVE6S100	*At. caldus*	Batch+S	Soluble cellular fraction S100	Rb	Rivas *et al.*, 2008
84	IVE7C1	*Halothiobacillus neapolitanus*	Batch+S	Whole cells	Rb	Rivas *et al.*, 2011
85	IVE8C1	*Acidimicrobium ferrooxidans*	Biomass from DSM N°10331	Whole cells	Rb	This work
86	IVE8S2	*Acidimicrobium ferrooxidans*	Biomass from DSM N°10331	Supernatant from EDTA wash	Rb	This work
87	IVF1S1	*Shewanella gelidimarina*	Batch (Marine broth 15°C)	Culture supernatant	Rb	Rivas *et al.*, 2008
88	IVF2C1	*S. gelidimarina*	Batch (Marine broth 4°C)	Whole cells	Rb	Rivas *et al.*, 2008
89	IVF2S2a	*S. gelidimarina*	Batch (Marine broth 4°C)	Supernatant from EDTA wash	Rb	Rivas *et al.*, 2008
90	IVF2S2b	*S. gelidimarina*	Batch (Marine broth 4°C)	Supernatant from EDTA wash	Rb	Rivas *et al.*, 2008
91	IVF2C2	*S. gelidimarina*	Batch (Marine broth 4°C)	Insoluble cell pellet from S100	Rb	Rivas *et al.*, 2008
92	IVF2S100	*S. gelidimarina*	Batch (Marine broth 4°C)	Soluble cellular fraction S100	Rb	Rivas *et al.*, 2008
93	IVF3C2	*Psychroserpens burtonensis*	Batch (Marine broth 15°C)	Insoluble cell pellet from S100	Rb	Rivas *et al.*, 2008
94	IVF4C1	*P. burtonensis*	Batch (Marine broth 4°C)	Whole cells	Rb	Rivas *et al.*, 2008
95	IVF4S1	*P. burtonensis*	Batch (Marine broth 4°C)	Culture supernatant	Rb	Rivas *et al.*, 2008
96	IVF4S2a	*P. burtonensis*	Batch (Marine broth 4°C)	Supernatant from EDTA wash	Rb	Rivas *et al.*, 2008
97	IVF4S2b	*P. burtonensis*	Batch (Marine broth 4°C)	Supernatant from EDTA wash	Rb	Rivas *et al.*, 2008
98	IVF4S100	*P. burtonensis*	Batch (Marine broth 4°C)	Soluble cellular fraction S100	Rb	Rivas *et al.*, 2008
99	IVF5C1	*Psychrobacter frigidicola*	Batch (Harpo's medium 15°C)	Whole cells	Rb	Rivas *et al.*, 2008
100	IVF5S1	*Ps. frigidicola*	Batch (Harpo's medium 15°C)	Culture supernatant	Rb	Rivas *et al.*, 2008
101	IVF5C2	*Ps. frigidicola*	Batch (Harpo's medium 15°C)	Insoluble cell pellet from S100	Rb	Rivas *et al.*, 2008
102	IVF5S100	*Ps. frigidicola*	Batch (Harpo's medium 15°C)	Soluble cellular fraction S100	Rb	Rivas *et al.*, 2008
103	IVF6C1	*Cryobacterium psychrophilum*	Batch (TSA)	Whole cells	Rb	Rivas *et al.*, 2008
104	IVF6S1	*C. psychrophilum*	Batch (TSA)	Culture supernatant	Rb	Rivas *et al.*, 2008
105	IVF6S2	*C. psychrophilum*	Batch (TSA)	Supernatant from EDTA wash	Rb	Rivas *et al.*, 2008
106	IVF6C2	*C. psychrophilum*	Batch (TSA)	Insoluble cell pellet from S100	Rb	Rivas *et al.*, 2008
107	IVF6S100	*C. psychrophilum*	Batch (TSA)	Soluble cellular fraction S100	Rb	Rivas *et al.*, 2008
108	IVF7C1	*Colwellia psychrerythraea*	Bath culture (Marine broth)	Whole cells	Rb	Rivas *et al.*, 2011
109	IVF7S1	*C. psychrerythraea*	Bath culture (Marine broth)	Culture supernatant	Rb	This work
110	IVF7S2	*C. psychrerythraea*	Bath culture (Marine broth)	Supernatant from EDTA wash	Rb	This work
111	IVG1C1	*Acidocella aminolytica* DSM 11237	Batch (DSMZ medium N°269)	Whole cells	Rb	Rivas *et al.*, 2011
112	IVG2C_185	*Acidiphilium* spp.	Batch (DSMZ medium N°269)	Whole cells	Rb	This work
113	IVG2C1	*Acidiphilium* sp.	Batch (DSMZ medium N°269)	Whole cells	Rb	Rivas *et al.*, 2011
114	IVG3C1	*Acidobacterium capsulatum* DSM 11244	Batch (DSMZ medium N°269)	Whole cells	Rb	Rivas *et al.*, 2011
115	IVG4C1	*Thermus scotoductus*	Batch (TYG)	Whole cells	Rb	Rivas *et al.*, 2011
116	IVG4C2	*T. scotoductus*	Batch (TYG)	Insoluble cell pellet from S100	Rb	Rivas *et al.*, 2011
117	IVG5C1	*Sulfobacillus acidophilus*	Biomass from DSM No 10332	Whole cells	Rb	Rivas *et al.*, 2011
118	IVG6C1	*T. termophilus*	Batch (TYG)	Whole cells	Rb	This work
119	IVH1C1	*Bacillus subtilis* (spores)	Batch (Schaeffer medium)	Whole spores	Rb	Fernández-Calvo *et al.*, 2006
120	IVI1C1	*Pseudomonas putida*	Batch (LB)	Whole cells	Rb	Rivas *et al.*, 2008

(*continued*)

Table 2. (Continued)

Ab No	Ab name	Source/Strain	Sample/Culture conditions	Immunogen/Fraction	Host	Supp. References
121	IVI1C2	*P. putida*	Batch (LB)	Insoluble cell pellet from S100	Rb	Rivas *et al.*, 2008
122	IVI1S100	*P. putida*	Batch (LB)	Soluble cellular fraction S100	Rb	Rivas *et al.*, 2008
123	IVI1RB	*P. putida*	Batch (LB)	Ribosome fraction	Rb	Rivas *et al.*, 2008
124	IVI2C1	*Bacillus* spp. (environ. isol.)*	Batch (LB)	Whole cells	Rb	Rivas *et al.*, 2008
125	IVI2S2	*Bacillus* spp. (environ. isol.)*	Batch (LB)	Supernatant from EDTA wash	Rb	Rivas *et al.*, 2008
126	IVI2C2	*Bacillus* spp. (environ. isol.)*	Batch (LB)	Insoluble cell pellet from S100	Rb	Rivas *et al.*, 2008
127	IVI2S100	*Bacillus* spp. (environ. isol.)*	Batch (LB)	Soluble cellular fraction S100	Rb	Rivas *et al.*, 2008
128	IVI3C1	*Shewanella oneidensis*	Batch (LB)	Whole cells	Rb	Rivas *et al.*, 2008
129	IVI3S2	*S. oneidensis*	Batch (LB)	Supernatant from EDTA wash	Rb	Rivas *et al.*, 2008
130	IVI3C2	*S. oneidensis*	Batch (LB)	Insoluble cell pellet from S100	Rb	Rivas *et al.*, 2008
131	IVI3S100	*S. oneidensis*	Batch (LB)	Soluble cellular fraction S100	Rb	Rivas *et al.*, 2008
132	IVI4C1	*Burkholderia fungorum*	Batch (LB)	Whole cells	Rb	Rivas *et al.*, 2008
133	IVI4S2	*B. fungorum*	Batch (LB)	Supernatant from EDTA wash	Rb	Rivas *et al.*, 2008
134	IVI4C2	*B. fungorum*	Batch (LB)	Insoluble cell pellet from S100	Rb	Rivas *et al.*, 2008
135	IVI4S100	*B. fungorum*	Batch (LB)	Soluble cellular fraction S100	Rb	Rivas *et al.*, 2008
136	IVI5C1	*S. oneidensis*	Anaerobic (fumarate)	Whole cells	Rb	Rivas *et al.*, 2008
137	IVI5S1	*S. oneidensis*	Anaerobic (fumarate)	Culture supernatant	Rb	Rivas *et al.*, 2008
138	IVI5C2	*S. oneidensis*	Anaerobic (fumarate)	Insoluble cell pellet from S100	Rb	Rivas *et al.*, 2008
139	IVI5S100	*S. oneidensis*	Anaerobic (fumarate)	Soluble cellular fraction S100	Rb	Rivas *et al.*, 2008
140	IVI6C3	*Azotobacter vinelandii*	Batch culture (LB)	EDTA washed cells (sonicated)	Rb	Rivas *et al.*, 2008
141	IVI7C1	*B. subtilis* 168	Batch culture (LB) vegetative cells	Whole cells	Rb	Rivas *et al.*, 2008
142	IVI8C1	*B. subtilis* 3610	Biofilm	Whole cells	Rb	Rivas *et al.*, 2008
143	IVI8S1	*B. subtilis* 3610	Biofilm	Culture supernatant	Rb	Rivas *et al.*, 2008
144	IVI9C1	*Deinococcus radiodurans*	Biomass from DSMZ No 20539	Whole cells	Rb	Rivas *et al.*, 2008
145	IVI10C1	*Desulfovibrio vulgaris (vulgaris)*	Biomass from DSMZ No 644	Whole cells	Rb	Rivas *et al.*, 2008
146	IVI11C1	*Geobacter sulfurreducens*	Biomass from DSMZ No 12127	Whole cells	Rb	Rivas *et al.*, 2008
147	IVI12C1	*Geobacter metallireducens*	Biomass from DSMZ No 7210	Whole cells	Rb	Rivas *et al.*, 2008
148	IVI13C1	*Thermotoga maritima*	Biomass from DSMZ No 3109	Whole cells	Rb	Rivas *et al.*, 2008
149	IVI14C1	*Verrucomicrobium spinosum*	Biomass from DSMZ No 4136	Whole cells	Rb	Rivas *et al.*, 2008
150	IVI15C1	*Methylomicrobium capsulatum*	Biomass from DSMZ No 6130	Whole cells	Rb	Rivas *et al.*, 2008
151	IVI16C1	*Planctomyces limnophilus*	Biomass from DSMZ No 3776	Whole cells	Rb	Rivas *et al.*, 2008
152	IVI17C1	*Hydrogenobacter thermophilus*	Biomass from DSMZ No 6534	Whole cells	Rb	Rivas *et al.*, 2008
153	IVI19C1	*Desulfosporosinus meridiei*	Biomass from DSM No 13257	Whole cells	Rb	Rivas *et al.*, 2011
154	IVI20C1	*Salinibacter ruber* M8	Batch (SW25% marine salt)	Whole cells	Rb	Rivas *et al.*, 2011
155	IVI21C1	*S. ruber* PR1	Batch (SW25% marine salt)	Whole cells	Rb	Rivas *et al.*, 2011
156	IVI21C2	*S. ruber* PR1	Batch (SW25% marine salt)	Insoluble cell pellet from S100	Rb	Rivas *et al.*, 2011
157	IVI21S1	*S. ruber* PR1	Batch (SW25% marine salt)	Culture supernatant	Rb	This work
158	IVJ1C1	*Haloferax mediterranei*	Batch (SW25% marine salt)	Whole cells	Rb	Rivas *et al.*, 2008
159	IVJ2C1	*Methanococcoides burtonii*	Biomass from DSMZ No 6242	Whole cells	Rb	Rivas *et al.*, 2008
160	IVJ3C1	*Thermoplasma acidophilum*	Biomass from DSMZ No 1728	Whole cells	Rb	Rivas *et al.*, 2008
161	IVJ4C1	*Methanobacterium formicicum*	Biomass from DSMZ No 1535	Whole cells	Rb	Rivas *et al.*, 2008
162	IVJ5C1	*Methanosarcina mazeii*	Biomass from DSMZ No 3647	Whole cells	Rb	Rivas *et al.*, 2008
163	IVJ6C1	*Pyrococcus furiosus*	Biomass from DSM No 3638	Whole cells	Rb	Rivas *et al.*, 2011
164	IVJ8C1	*Halorubrum* sp.	Batch (SW25% marine salt)	Whole cells	Rb	Rivas *et al.*, 2011
165	IVJ9C1	*Halobacterium* sp.	Batch (SW25% marine salt)	Whole cells	Rb	Rivas *et al.*, 2011

(*continued*)

Table 2. (Continued)

Ab No	Ab name	Source/Strain	Sample/Culture conditions	Immunogen/Fraction	Host	Supp. References
166	A-Ecoli1	*Escherichia coli*	*E. coli* culture	All serotypes	Rb	US Biological (E3500-26)
167	A-Hpylori	*Helicobacter pylori*	Batch culture (ATCC 43504)	Whole cells	Rb	BIODESIGN (B65660R)
168	A-Lmono	*L. monocytogenes*	Batch culture (ATCC 43251)	Whole cells	Rb	BIODESIGN (B65420R)
169	A-Mycob	*Mycobacterium* genus	Batch culture *M. tuberculosis*	Genus-specific antigens extract	Rb	BIODESIGN (B47827R)
170	A-Paer	*P. aeruginosa*	Batch culture (*P. aeruginosa*)	Outer membrane protein extract	Gpig	BIODESIGN (B47578G)
171	A-Salm	*Salmonella* sp. (O+H Ags)	Batch culture	Mix *S. enteritidis*, typhym., heidelburg	Rb	BIODESIGN (B65701R)
172	A-G+Ag	Gram-positive antigen	Culture	Gram-positive antigen	M(Mab)	BIODESIGN (C11333M)
173	A-G+Bac	Gram-positive Bacteria	Culture	Lipoteichoic acid Gram-positives	M(Mab)	BIODESIGN (C65380M)
174	A-PG	Peptidoglycan	Culture (*Streptococcus mutans*)	Insoluble PG extract obtained by TCA	M(Mab)	CHEM. INTER. (MAB997)
175	A-lipidA	Lipid A (*E. coli* O157)	Culture	Whole cells prep of lipid A	Goat	BIODESIGN (B65692G)
176	A-LTA	Lipoteichoic acid	Culture	Native *Streptococcus pyrogenes*	Rb	BIODESIGN (B30103R)
177	A-NAG	N-Acetylglucosamine	NAG on proteins	NAG-KLH conjugated	M(Mab)	BIODESIGN (H67108M)
178	A-DNA1	ss, dsDNA	Bovine ss, dsDNA	Calf thymus DNA	M(Mab)	US Biological (D3878-05)
179	A-DNA2	DNA102 (human)	dsDNA	Autoimmune	Hu	Schweitzer *et al.*, 2005
180	A-dsDNA(hu)	dsDNA (human plasma)	dsDNA	Autoimmune	Hu	BIODESIGN (K07112H)
181	A-RNApII	RNA polymerase II	Eukaryotic RNApol	Wheat germ RNApol II (purified)	M(Mab)	BIODESIGN (M55701M)
182	A-GroEL	GroEL (*E. coli*)	Recombinant	GroEL (purified)	Rb	Sigma-Aldrich (G6532)
183	A-Hsp70	HSP-70	Batch culture (*M. tuberculosis*)	HSP-70 (purified protein)	M(Mab)	BIODESIGN (H86313M)
184	A-Lasnase	L-Asparaginase (*E. coli*)	Batch culture	L-Asparaginase (purified)	Rb	BIODESIGN (K59171R)
185	A-BGal	beta d Galactosidase (*E. coli*)	Batch culture	Beta d Galactosidase (purified)	Rb	BIODESIGN (K03450R)
186	A-GluOxid	Glucose oxidase	Batch culture (*Aspergillus niger*)	Glucose oxidase (purified)	Rb	BIODESIGN (K59137R)
187	A-GST	Glutathione-*S*-transferase	Recombinant (*S. japonicum*)	GST (purified)	Rb	Sigma-Aldrich (G7781)
188	A-Stv	Streptavidin	Culture (*Streptomyces avidinii*)	Streptavidin (purified)	Rb	Sigma-Aldrich (S6390)
189	A-Thio	Thioredoxin (*E. coli*)	Recombinant	Thioredoxin (purified)	Rb	Sigma-Aldrich (T0803)
190	A-Bglu	*B. subtilis* beta-glucanase	Recombinant (*B. subtilis*)	Beta-glucanase SDS-PAGE purified	Rb	Rivas *et al.*, 2008
191	A-Csn	*B. subtilis* chitosanase	Recombinant (*B. subtilis*)	Csn SDS-PAGE purified	Rb	Rivas *et al.*, 2008
192	A-Hfer	Human ferritin	From human liver	Ferritin (purified)	M(Mab)	BIODESIGN (H53715)
193	A1484	NIFH3 peptide	seq. AKGILKYANSGGVRL	KLH conjugate	Rb	Fernández-Calvo *et al.*, 2006
194	A1485	NIFD2 peptide	seq. YRSMNYISRHMEEKY	KLH conjugate	Rb	Fernández-Calvo *et al.*, 2006
195	A1487	HSCA2 peptide	seq. TFTIDANGILDVRAL	KLH conjugate	Rb	Fernández-Calvo *et al.*, 2006
196	A1490	FDX2 peptide	seq. HVIITEGFDNLSPME	KLH conjugate	Rb	Fernández-Calvo *et al.*, 2006
197	A1492	GLNB2 peptide	seq. VETALRIRTGETGDA	KLH conjugate	Rb	Fernández-Calvo *et al.*, 2006
198	A1494	MODA2 peptide	seq. MLAPLHKKIVYANTL	KLH conjugate	Rb	Fernández-Calvo *et al.*, 2006
199	A1496	NIFS2 peptide	seq. LPVNKEGRVEIETLK	KLH conjugate	Rb	Fernández-Calvo *et al.*, 2006
200	LectinPo	Lectin potato protein (not Ab)	SDS-PAGE purified protein	Not applicable	—	CALBIOCHEM (431788)
201	A-cAMP1	Cyclic AMP	Cyclic AMP	3′-5′-cAMP-2′-BSA conjugated	Rb	Sigma-Genosys (A0670)
202	A-cAMP2	Cyclic AMP	Human cAMP	Succinylated cAMP-BSA conjugated	Rb	US Biological (C8450-05)
203	A-cAMP3	Cyclic AMP	Cyclic AMP	Succinylated cAMP-BSA conjugated	Sheep	BIODESIGN (Q55101S)
204	A-Asp	Aspartate	Purified Asp	Asp-KLH conjugated	Rb	Sigma-Aldrich (A9684)
205	A-Glu	Glutamate	Purified Glu	Glu-KLH conjugated	Rb	Sigma-Aldrich (G6642)

(*continued*)

Table 2. (Continued)

Ab No	Ab name	Source/Strain	Sample/Culture conditions	Immunogen/Fraction	Host	Supp. References
206	A-Trp	Tryptophan	Tryptophan	Trp-glutaraldehyde-Poly-lysine	Rb	US Biological (T9013-05)
207	A-polyHis	PolyHistidine	Poly-His	His-Tagged fusion protein	M(Mab)	Sigma-Aldrich (H1029)
208	A-Cortisol	Cortisol	Cortisol	Cortisol-21-hemisucc.-Thyroglobulin	Rb	Sigma-Aldrich (C8409)
209	A-Estrad1	Estradiol	17-beta-Estradiol	17-beta-Estradiol-BSA	M(Mab)	BIODESIGN (E86022M)
210	A-Estrad2	Estradiol	17-beta-Estradiol	Estradiol-17-beta-6-BSA conjugated	M(Mab)	BIODESIGN (H31100M)
211	A-Pen	Penicillin	Penicllin and derivatives	Penicillin-BSA conjugated	M(Mab)	BIODESIGN (G13011M)
212	A-Tc	Tetracycline	Tetracycline	Tetracycline-BSA	Rb	US Biological (T2965-05)
213	A-VitB12	Vitamin B12	Cyanocobalamine	Vitamin B12-BSA conjugated	Rb	US Biological (C8400-10)
214	A-Atrazine	Atrazine	Atrazine	Atrazine-BgG	Rb	BIODESIGN (K82102R)
215	A-HBVAg	Hepatitis B virus surface Ag	Hepatitis B virus surface antigen	Highly purified Hepatitis B antigen	Goat	ABCAM (ab9216)
216	A-Surfactin_N	Surfactin	Sigma S3523	Surfactin-Amine-BSA	Rb	This work
217	A-ASB_11362	*Archaeoglobus fulgidus*	ATP synthase, subunit B (Archaea)	Purified recombinant polipeptide	Rb	This work
218	A-ASF1_11355	*Thermotoga maritima*	ATP synthase F1, subunit Alpha (Bacteria)	Purified recombinant polipeptide	Rb	This work
219	A-BaFER	Bacterioferritin	Bacterioferritin	Purified recombinant polipeptide	Rb	Rivas *et al.*, 2011**
220	A-CrReTs_977	*T. scotoductus*	Chromate reductase (membrane)	Purified recombinant polipeptide	Rb	Rivas *et al.*, 2011
221	A-CspA-11357	*P. putida*	Cold shock protein A	Purified recombinant polipeptide	Rb	This work
222	A-DsrA-11365	DsrA (*Archaeoglobus fulgidus*)	Dissimilatory sulfite reductase	Purified recombinant polipeptide	Rb	This work
223	A-DsrB_11368	DsrB (*Archaeoglobus fulgidus*)	Dissimilatory sulfite reductase	Purified recombinant polipeptide	Rb	This work
224	A-EFG_11359	*Thermotoga maritima*	Elongation factor G	Purified recombinant polipeptide	Rb	This work
225	A-FdhF	FDHF (*E. coli* K12)	Selenopolypeptide sub. Formate DeHase H	Purified recombinant polipeptide	Rb	This work
226	A-FeReTs_983	Iron reductase (*T. scotoductus*)	Iron reductase	Purified recombinant polipeptide	Rb	This work
227	A-HtpG	HtpG (*Nostoc* PCC73102)	HtpG homologous to HSP90	Purified recombinant polipeptide	Rb	This work
228	A-HupL	HupL (*At. ferrooxidans*)	Ni-Fe membrane hydrogenase L chain	Purified recombinant polipeptide	Rb	This work
229	A-HupS	HupS (*L. ferrooxidans*)	Ni-Fe membrane hydrogenase S chain	Purified recombinant polipeptide	Rb	This work
230	A-HyfG	HyfG (*E. coli*)	Hydrogenase 4, component B	Purified recombinant polipeptide	Rb	This work
231	A-McrB_11378	McrB (*Methanococcoides burtonii*)	Methyl CoM reductase I, B subunit	Purified recombinant polipeptide	Rb	This work
232	A-NADH_11363	NuoF (*P. putida*)	NADH dehydrogenase I (quinone)	Purified recombinant polipeptide	Rb	This work
233	A-NifD_11466	NifD (*G. metallireducens*)	NifD protein	Purified recombinant polipeptide	Rb	This work
234	A-NirS_11369	NirS (*P. aeruginosa*)	Nitrite reductase	Purified recombinant polipeptide	Rb	This work
235	A-NOR1_11375	NOR1 (*N. hamburgensis*)	Nitrite oxidoreductase Beta subunit	Purified recombinant polipeptide	Rb	This work
236	A-NRA-11912	NRA (*G. metallireducens*)	Nitrate reductase subunit Alpha	Purified recombinant polipeptide	Rb	This work
237	A-OmpA	OmpA (*E. coli*)	OmpA membrane protein	Purified recombinant polipeptide	Rb	This work
238	A-OppA	OppA (*Bacillus subtilis*)	Oligopeptide binding protein sub A	Purified recombinant polipeptide	Rb	This work
239	A-PfuDPS	DPS (*Pyrococcus furiosus*)	Fe-binding and storage protein DpS	Purified recombinant polipeptide	Rb	Rivas *et al.*, 2011**
240	A-PfuFER	Ferritin (*P. furiosus*)	Ferritin Fe-binding and storage protein	Purified recombinant polipeptide	Rb	Rivas *et al.*, 2011**
241	A-RbcL_RB11374	RbcL (*At. ferrooxidans*)	Rubisco large subunit	Purified recombinant polipeptide	Rb	This work
242	A-Rusticyanin	Rusticyanin (*At. ferooxidans*)	Rusticyanin	Purified recombinant polipeptide	Rb	This work
243	A-SsoDPS	DPS (*Sulfolobus solfataricus*)	Fe-binding and storage protein DpS	Purified recombinant polipeptide	Rb	Rivas *et al.*, 2011**
244	A-ABCtrans	ABC transporter (*T. scotoductus*)	ABC-transporter protein	Purified recombinant polipeptide	Rb	Rivas *et al.*, 2011
245	A-ApsA-11754	ApsA (*Desulfovibrio desulfuricans*)	HMMLREMREGRGPIYC	Conjugate	Rb	This work

(*continued*)

Table 2. (Continued)

Ab No	Ab name	Source/Strain	Sample/Culture conditions	Immunogen/Fraction	Host	Supp. References
246	A-BfR	BFR (*D. desulfuricans*)	CAENFAERIKELFFEP	Conjugate	Rb	This work
247	A-CcdA	CcdA (*Geobacter sulfurreducens*)	CLLGEKRLQVHRKPAGY	Conjugate	Rb	This work
248	A-cydA-11758	CydA (*S. oneidensis*)	YILKKRDLPFARRSFAC	Conjugate	Rb	This work
249	A-DhnA1	DhnA (*Nostoc* PCC73102)	LRNNAFKQDKDYHLAC	Conjugate	Rb	This work
250	A-DhnA2	DhnA (*Nostoc* PCC73102)	SGRKAFQRPFEEGVKLC	Conjugate	Rb	This work
251	A-FtsZ	FtsZ *Pseudomonas putida*	CPFEGRKRMQIADEGIR	Conjugate	Rb	This work
252	A-GGDEF_11760	Sensory box/GGDEF Domain	IDLDEFKRIN(DT)FGHKEGDKVC	Conjugate	Rb	This work
253	A-Groel	GroEL (*G. metallireducens*)	ETEMKEKKARVEDALC	Conjugate	Rb	This work
254	A-ICDH_11755	ICDH-NAD (*C. hydrogenoformans*)	VL(ES)IKKNKVALKGPC	Conjugate	Rb	This work
255	A-IsiA1	IsiA, PSII (*Nostoc* PCC73102)	EISRYKPEIPMGEQGC	Conjugate	Rb	This work
256	A-IsiA2	IsiA, PSII (*Nostoc* PCC73102)	FHFEWNDPKLGLILC	Conjugate	Rb	This work
257	A-Ktrans_11750	K+-transporter (*G. metallireducens*)	LAMSLGRKGEGGTIVC	Conjugate	Rb	This work
258	A-NifD1_12288	NifD1 (*Burkholderia xenovorans*)	VFDKADPDKRPDFVSC	Conjugate	Rb	This work
259	A-NifD3_12289	NifD3 (*B. xenovorans*)	VFGGDKKLDKIIDEIC	Conjugate	Rb	This work
260	A-NifH1_12291	NifH1 (*B. xenovorans*)	CNERQTDKELELAEAL	Conjugate	Rb	This work
261	A-NifH2_12293	NifH2 (*B. xenovorans*)	EFAPESKQAEEYRQLC	Conjugate	Rb	This work
262	A-OmcS	OmcS (*G. sulfurreducens*)	CHDPHGKYRRFVDGSI	Conjugate	Rb	This work
263	A-PhaC1	PhaC (*Pseudomonas putida*)	CSLAPDSDDRRFNDPA	Conjugate	Rb	This work
264	A-PhaC2	PhaC (*P. putida*)	CLGERAGALKKAPTRL	Conjugate	Rb	This work
265	A-PhcA1	PhcA (*Nostoc* PCC73103)	NTELQSARGRYERAAC	Conjugate	Rb	This work
266	A-PhcA2	PhCA (*Nostoc* PCC73104)	TPGPQFAADSRGKSKC	Conjugate	Rb	This work
267	A-PufM1	PufM (*Rhodospirillum rubrum*)	SRLGGDREVEQITDRC	Conjugate	Rb	This work
268	A-PufM2	PufM (*Rhodospirillum rubrum*)	SRLGGDREVEQITDRC	Conjugate	Rb	This work
269	A-RRO	Rubredoxin (*D. desulfuricans* G20)	CHTQDETMKALEIKKDV	Conjugate	Rb	This work
270	A-SodA	SodA (*G. sulfurreducens*)	CMLDYGLKRPDYIEAF	Conjugate	Rb	This work
271	A-SodF	SodF (*G. sulfurreducens*)	CARIDKDFGSFDKFKEE	Conjugate	Rb	This work
272	A-WshR	Water stress protein (*P. putida* F1)	CVRFTDEGKLDLPKGT	Conjugate	Rb	This work
273	A-AeKaC_S	AEKAC peptide	AEKAC-synthetic	Conjugate	Rb	This work
274	A-EPS_SP	Exopolysaccharides	Solar saltern (Santa Pola, Alicante, Spain)	EPS extract	Rb	This work
275	A-LPS_N	LPS (*Pseudomonas* sp.)		LPS-BSA	Rb	This work
276	A-LipidA_43	LipidA		Lipid A	Mab	Hycult biotech. (HM2046)
277	A-AMP_N	AMP		AMP-OH-BSA	Rb	This work
278	A-cAMP_N	cAMP		cAMP-OH-BSA	Rb	This work
279	A-cAMP_sh	cAMP		Succinylated cAMP-BSA	Rb	Abcam (ab832)
280	A-cGMP(bio)	cGMP		2′O-succinyl guanosine-3′,5′ cGMP	Rb	MBL, Inc. (JM-3568-100)
281	A-cGMP_N	cGMP		cGMP-OH-BSA	Rb	This work
282	A-CoA_S	Coenzyme A		CoA-SH-BSA	Rb	This work
283	A-Digoxin	Digoxin		Digoxin-KLH	Mab	SIGMA (D 8156)
285	A-dinitroph.	Dinitrophenol		Dinitrophenol-BSA	Rb	SIGMA (D 9656)
286	A-cGMP(ups)	cGMP		2′-Monosuccinyl cyclic GMP-KLH	Rb	UPSTATE
287	A-GMP_N	GMP		GMP-OH-BSA	Rb	This work

(*continued*)

Table 2. (Continued)

Ab No	Ab name	Source/Strain	Sample/Culture conditions	Immunogen/Fraction	Host	Supp. References
288	A-Proto IX_N	Protoporphyrin IX		Protophorphyrin IX-OH-BSA	Rb	This work
289	A-Thiamine	Thiamine		Thiamine-BSA	Rb	US Biological (T5004)
290	A-Arg	Arginine	Arginine	Asymmetric NG-NG-dimethyl arginine	Rb	Santa Cruz Biotech.sc-57626
292	A-Ala_N	Ala		Ala-NH2-BSA	Rb	This work
294	A-aa_N	Amino acids		Cys-SH-BSA	Rb	This work
295	A-Gly_N	Gly		Gly-NH2-BSA	Rb	This work
296	A-His_N	His		His-NH2-BSA	Rb	This work
298	A-Phe_N	Phe		Phe-NH2-BSA	Rb	This work
299	A-Tyr_N	Tyr		Tyr-NH2-BSA	Rb	This work
300	A-Val_N	Val		Val-NH2-BSA	Rb	This work
301	P-139	Pre-Immune serum	IgG fraction (protein A purified)	Pre-Immune serum	Rb	Rivas *et al.*, 2008
302	P-1496	Pre-Immune serum	IgG fraction (protein A purified)	Pre-Immune serum	Rb	Rivas *et al.*, 2008
303	P-IA1S2	Pre-Immune serum	IgG fraction (protein A purified)	Pre-Immune serum	Rb	Rivas *et al.*, 2008
304	P-IA1C1	Pre-Immune serum	IgG fraction (protein A purified)	Pre-Immune serum	Rb	Rivas *et al.*, 2008
305	p-IA2S1	Pre-Immune serum	IgG fraction (protein A purified)	Pre-Immune serum	Rb	This work
306	p-IA3C1	Pre-Immune serum	IgG fraction (protein A purified)	Pre-Immune serum	Rb	This work
307	P-IC1S1	Pre-Immune serum	IgG fraction (protein A purified)	Pre-Immune serum	Rb	Rivas *et al.*, 2008
308	P-IC1C1	Pre-Immune serum	IgG fraction (protein A purified)	Pre-Immune serum	Rb	Rivas *et al.*, 2008
309	p-IC4C1	Pre-Immune serum	IgG fraction (protein A purified)	Pre-Immune serum	Rb	This work
310	p-IC7C1	Pre-Immune serum	IgG fraction (protein A purified)	Pre-Immune serum	Rb	This work
311	P-IC8C1	Pre-Immune serum	IgG fraction (protein A purified)	Pre-Immune serum	Rb	Rivas *et al.*, 2008
312	p-IC9C1	Pre-Immune serum	IgG fraction (protein A purified)	Pre-Immune serum	Rb	This work
313	P-ID4S2	Pre-Immune serum	IgG fraction (protein A purified)	Pre-Immune serum	Rb	Rivas *et al.*, 2008
314	P-IVE1C1	Pre-Immune serum	IgG fraction (protein A purified)	Pre-Immune serum	Rb	Rivas *et al.*, 2008
315	P-IVE3C1	Pre-Immune serum	IgG fraction (protein A purified)	Pre-Immune serum	Rb	Rivas *et al.*, 2008
316	P-IVE4C1	Pre-Immune serum	IgG fraction (protein A purified)	Pre-Immune serum	Rb	Rivas *et al.*, 2008
317	P-IVE5C1	Pre-Immune serum	IgG fraction (protein A purified)	Pre-Immune serum	Rb	Rivas *et al.*, 2008
318	P-IVE6C1	Pre-Immune serum	IgG fraction (protein A purified)	Pre-Immune serum	Rb	Rivas *et al.*, 2008
319	P-IVF2C1	Pre-Immune serum	IgG fraction (protein A purified)	Pre-Immune serum	Rb	Rivas *et al.*, 2008
320	p-IVG2C1	Pre-Immune serum	IgG fraction (protein A purified)	Pre-Immune serum	Rb	This work
321	p-IVG4C1	Pre-Immune serum	IgG fraction (protein A purified)	Pre-Immune serum	Rb	This work
322	P-IVI2C1	Pre-Immune serum	IgG fraction (protein A purified)	Pre-Immune serum	Rb	Rivas *et al.*, 2008
323	P-IVI8C1	Pre-Immune serum	IgG fraction (protein A purified)	Pre-Immune serum	Rb	Rivas *et al.*, 2008
324	p-IVI10C1	Pre-Immune serum	IgG fraction (protein A purified)	Pre-Immune serum	Rb	This work
325	p-IVI120C1	Pre-Immune serum	IgG fraction (protein A purified)	Pre-Immune serum	Rb	This work
326	p-ABCtrans	Pre-Immune serum	IgG fraction (protein A purified)	Pre-Immune serum	Rb	This work
327	p-CrReTs-977	Pre-Immune serum	IgG fraction (protein A purified)	Pre-Immune serum	Rb	This work
328	p-FeReTs-983	Pre-Immune serum	IgG fraction (protein A purified)	Pre-Immune serum	Rb	This work
329	p-FeReTs-984	Pre-Immune serum	IgG fraction (protein A purified)	Pre-Immune serum	Rb	This work
330	p-pool	Pre-Immune sera pool	IgG fraction (protein A purified)	Pre-Immune sera pool	Rb	Rivas *et al.*, 2008

C1, cellular fraction; C2, insoluble cell pellet from S100; C3, EDTA washed cells; S1, culture supernatant; S2, supernatant from EDTA wash.
Rb, polyclonal antibodies from rabbit; M(Mab), monoclonal Abs from mouse; Mab, monoclonal antibody; Hu, human; Gpig, Guinea pig.
*Environmental isolated from Río Tinto (kindly provided by Felipe Gómez-Gómez).
**Antigens (purified proteins) were kindly provided by Dr. Trevor Douglas, Center for BioInspired Nanomaterials, Montana State University, Bozeman, MT.